Scheme 4

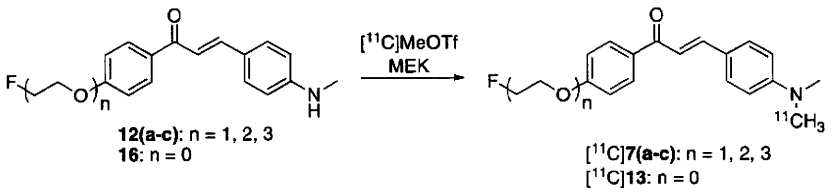

Scheme 5

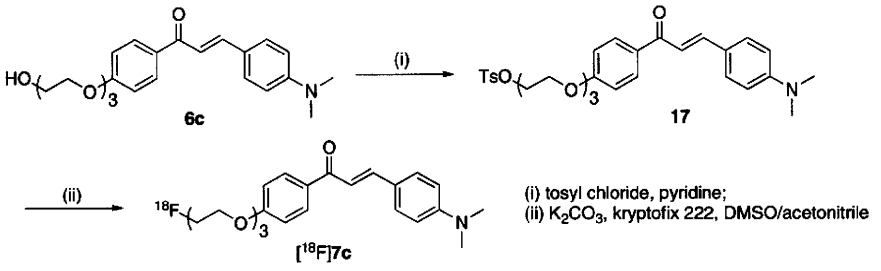

Table 1. Chemical Structures and Inhibition Constants of Fluorinated Chalcone Derivatives

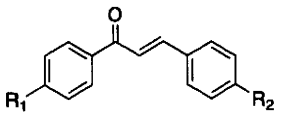

compd	R_1	R_2	K_i (nM)[a]
7a	FCH_2CH_2O	$N(CH_3)_2$	45.7 ± 7.1
7b	$F(CH_2CH_2O)_2$	$N(CH_3)_2$	20.0 ± 2.5
7c	$F(CH_2CH_2O)_3$	$N(CH_3)_2$	38.9 ± 4.2
11a	FCH_2CH_2O	NH_2	678.9 ± 21.7
11b	$F(CH_2CH_2O)_2$	NH_2	1048.0 ± 114.3
11c	$F(CH_2CH_2O)_3$	NH_2	790.0 ± 132.1
12a	FCH_2CH_2O	$NHCH_3$	197.1 ± 58.8
12b	$F(CH_2CH_2O)_2$	$NHCH_3$	216.4 ± 13.8
12c	$F(CH_2CH_2O)_3$	$NHCH_3$	470.9 ± 100.4
13	F	$N(CH_3)_2$	49.8 ± 6.2
15	F	NH_2	663.0 ± 88.3
16	F	$NHCH_3$	234.2 ± 44.0
DMIC	I	$N(CH_3)_2$	13.1 ± 3.0
IMPY			28.0 ± 4.1

[a] Inhibition constants (K_i, nM) of compounds for the binding of [^{125}I]DMIC to Aβ(1−42) aggregates. Values are the mean ± standard error of the mean for 4−9 independent experiments.

were readily synthesized from their *N*-normethyl precursors, **12(a−c)** and **16**, and [^{11}C]methyl triflate ([^{11}C]-MeOTf). Radiochemical yields of the final product were 28−35%, decay corrected to end of bombardment. Radiochemical purity was >99% with a specific activity of 22−28 GBq/μmol. The identity of [^{11}C]**7a**, [^{11}C]**7b**, [^{11}C]**7c**, and [^{11}C]**13** was confirmed by a comparison of HPLC retention times with the nonradioactive compounds (**7a**, **7b**, **7c**, and **13**). ^{18}F labeling of **7c** was performed on a tosyl precursor **17** undergoing a nucleophilic displacement reaction with the fluoride anion (Scheme 5). Radiolabeling with ^{18}F was successfully performed on the precursor to generate [^{18}F]**7c** with a radiochemical yield of 45% and radiochemical purity >99%. The identity of [^{18}F]**7c** was verified by a comparison of retention time with the nonradioactive compound. The specific activity of [^{18}F]**7c** was estimated to be 35 GBq/mmol at the end of synthesis.

Table 2. Biodistribution of Radioactivity after Injection of [^{11}C]**7a**, [^{11}C]**7b**, [^{11}C]**7c**, and [^{11}C]**13** in Normal Mice[a]

organ	2 min	10 min	30 min	60 min
		[^{11}C]**7a**		
blood	3.65 ± 0.37	2.73 ± 0.28	2.12 ± 0.18	2.22 ± 0.25
brain	6.01 ± 0.61	3.24 ± 0.39	2.57 ± 0.26	2.26 ± 0.41
		[^{11}C]**7b**		
blood	3.48 ± 0.56	2.28 ± 0.84	2.54 ± 0.96	1.44 ± 0.36
brain	4.73 ± 0.47	2.23 ± 0.18	1.14 ± 0.12	1.00 ± 0.19
		[^{11}C]**7c**		
blood	2.44 ± 0.25	1.52 ± 0.42	1.01 ± 0.15	0.68 ± 0.10
brain	4.31 ± 0.33	1.38 ± 0.16	0.64 ± 0.07	0.35 ± 0.03
		[^{11}C]**13**		
blood	2.61 ± 0.35	1.60 ± 0.25	0.39 ± 0.05	1.40 ± 0.20
brain	3.68 ± 0.35	1.53 ± 0.14	1.04 ± 0.15	1.04 ± 0.20

[a] Expressed as % of injected dose per gram. Each value represents the mean ± SD for 4−5 mice.

Table 3. Biodistribution of Radioactivity after Injection of [^{18}F]**7c** in Normal Mice[a]

organ	2 min	10 min	30 min	60 min
blood	2.09 ± 0.40	1.94 ± 0.18	2.35 ± 0.33	1.87 ± 0.26
brain	3.48 ± 0.47	1.52 ± 0.03	1.08 ± 0.09	1.07 ± 0.17
bone	1.80 ± 0.31	1.76 ± 0.15	2.98 ± 0.49	3.58 ± 0.41

[a] Expressed as % of injected dose per gram. Each value represents the mean ± SD for 4−5 mice.

Experiments in vitro to evaluate the affinity of the FPEG chalcones for Aβ aggregates were carried out in solutions of Aβ aggregates with [^{125}I]4-dimethylamino-4′-iodo-chalcone ([^{125}I]DMIC)[18] as the ligand (Table 1). The K_i values suggested that the binding to Aβ(1−42) aggregates was affected by substitution at the amino group at position 4 in the chalcone structure, not by the length of PEG introduced into the chalcone backbone. The fluorinated chalcones had binding affinity for Aβ(1−42) aggregates in the following order: the dimethyamino derivatives (**7a**, **7b**, **7c**, and **13**) > the monomethylamino derivatives (**12a**, **12b**, **12c**, and **16**) > the primary amino derivatives (**11a**, **11b**, **11c**, and **15**). The result of the binding experiments is consistent with that of previous reports.[16,19] In addition, the affinity of the dimethylamino

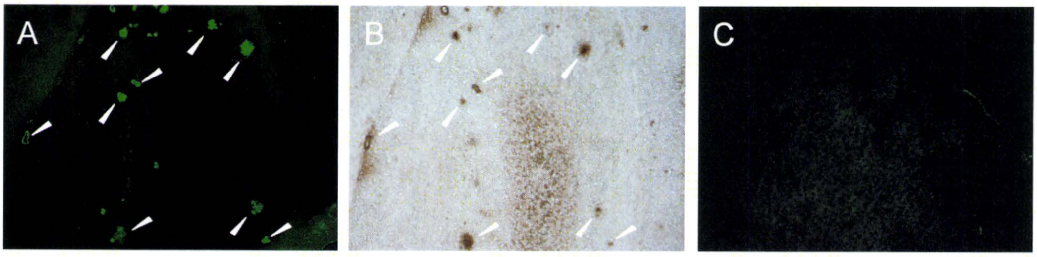

Figure 1. Neuropathological staining of 10 μm sections of a Tg2576 mouse brain (A and B) and aged normal brain (C). Fluorescent staining of compound **7c** in the Tg2576 mouse brain (A). Aβ immunostaining with antibody BC05 in the adjacent section (B). Fluorescent staining of compound **7c** in the age-matched control mouse brain (C).

derivatives was in the same range as that of the known compound, 6-iodo-2-(4′-dimethylamino)phenyl-imidazo[1,2-*a*]pyridine (IMPY), which is commonly used for inhibition assays.[22−25] We selected the dimethylamino derivatives (**7a**, **7b**, **7c**, and **13**), which showed the greatest affinity, for additional studies.

To evaluate brain uptake of the FPEG chalcones, biodistribution experiments were performed in normal mice with four ^{11}C-labeled FPEG chalcones ([^{11}C]**7a**, [^{11}C]**7b**, [^{11}C]**7c**, and [^{11}C]**13**) (Table 2). Because normal mice were used for the biodistribution experiments, no Aβ plaques were expected in the young mice; therefore the washout of probes from the brain should be rapid to obtain a higher signal-to-noise ratio earlier in the AD brain. Radioactivity after injection of the ^{11}C-labeled FPEG chalcones penetrated the blood−brain barrier, showing excellent uptake ranging from 3.7 to 6.0% ID/g brain at 2 min postinjection, a level sufficient for imaging Aβ plaques in the brain. In addition, they displayed good clearance from the normal brain with 2.3, 1.0, 0.35, and 1.0% ID/g at 60 min postinjection for [^{11}C]**7a**, [^{11}C]**7b**, [^{11}C]**7c**, and [^{11}C]**13**, respectively. These values were equal to 37.6, 21.1, 8.1, and 28.3% of the initial uptake peak for [^{11}C]**7a**, [^{11}C]**7b**, [^{11}C]**7c**, and [^{11}C]**13**, respectively. Compound **7c** with the fastest washout from the brain was labeled with ^{18}F and evaluated for its biodistribution in normal mice (Table 3). [^{18}F]**7c** displayed high uptake (3.48%ID/g) at 2 min postinjection, a level sufficient for imaging like [^{11}C]**7c**, and was cleared over the subsequent 10, 30, and 60 min. The radioactivity in the brain at 60 min postinjection was 1.07%ID/g, indicating that this [^{18}F]**7c** has favorable pharmacokinetics in the brain. Although we consider that a slight difference of the radioactivity pharmacokinetics between [^{11}C]**7c** and [^{18}F]**7c** could be attributable to the different physicochemical characteristics of their radiometabolites produced in the brain, the reason for this difference has remained unclear. Bone uptake at 60 min was measurable (3.58%ID/g), suggesting defluorination in vivo. Bone uptake has been observed for other ^{18}F tracers.[12,22−24] However, previous reports suggested that free fluoride was not taken up by brain tissue; therefore, the interference from free fluoride may be relatively low for brain imaging. A previous paper regarding the most promising ^{18}F-labeled agent **4** reported that it showed high uptake (7.77% ID/g at 2 min postinjection) and rapid clearance from the brain (1.61%ID/g at 60 min postinjection) with little accumulation in bone (1.77%ID/g at 60 min postinjection) in biodistribution experiments using normal mice.[12] The pharmacokinetics of **4** appear superior to that of [^{18}F]**7c**, but the good biological results obtained with [^{18}F]**7c** suggest that further investigation is warranted.

To investigate the ability of the fluorinated chalcones to bind to Aβ plaques in the AD model, fluorescent staining of sections of mouse brain were carried out with compound **7c** (Figure 1). We used Tg2576 transgenic mice as an animal model of Aβ plaque deposition, which express human APP695 with the K670N, M671L Swedish double mutation.[26] By 11−13 months of age, Tg2576 mice show prominent Aβ deposition in the cingulated cortex, entorhinal cortex, dentate gyrus, and CA1 hippocampal subfield and have been frequently used for the evaluation of specific binding of Aβ plaques in in vitro and in vivo experiments.[12,24,27−31] Many Aβ plaques were clearly stained with **7c**, as reflected by the affinity for the aggregates of synthetic Aβ(1−42) in in vitro competition assays (Figure 1A). The labeling pattern was consistent with that observed after immunohistochemical labeling by BC05, a specific antibody for Aβ (Figure 1B), while wild-type mouse brain displayed no significant accumulation of **7c** (Figure 1C). The results indicated that **7c** binds specifically to Aβ plaques in Tg2576 mice brain. A previous report suggested the configuration/folding of Aβ plaques in Tg2576 mice to be different from the tertiary/quaternary structure of Aβ plaques in AD brains.[30,32] In addition, the studies reported with **1** further indicate that the binding of **1** reflects the amount of Aβ plaques in human AD brain but not in Tg2576 mouse brain, and the detectability of Aβ plaques by **1** is dependent on the accumulation of specific Aβ subtypes.[28,29] Therefore, we considered that it should be essential to evaluate the binding affinity for Aβ plaques in human AD brains because our goal is to develop clinically useful probes for in vivo imaging of Aβ plaques in humans.

Next, we investigated the binding affinity of [^{18}F]**7c** for Aβ plaques by in vitro autoradiography in a human AD brain section (Figure 2A). The autoradiographic image of [^{18}F]**7c** showed high levels of radioactivity in some specific areas of the brain section. Furthermore, we confirmed that the hot spots of [^{18}F]**7c** in an AD brain section corresponded with those of in vitro thioflavin-S staining in the same brain section (Figure 2B). In contrast, no significant accumulation of [^{18}F]**7c** was observed in the region without Aβ plaques (Figure 2C). The results demonstrate the feasibility of using [^{18}F]**7c** as a probe for detecting Aβ plaques in the brain of AD patients with PET.

In conclusion, we reported novel FPEG chalcone derivatives, containing an end-capped fluoropolyethylene glycol as in vivo PET imaging agents for Aβ plaques in the brain. The FPEG chalcones with a dimethylamino group displayed greater affinity for synthetic Aβ aggregates than did the monomethylamino and primary amino derivatives. In biodistribution experiments using normal mice, ^{11}C-labeled FPEG chalcones displayed sufficient uptake for the imaging of Aβ plaques in the brain. [^{11}C]**7c** showed the fastest clearance from the brain, probably related to a low nonspecific binding. [^{18}F]**7c** also displayed high uptake in and good clearance from

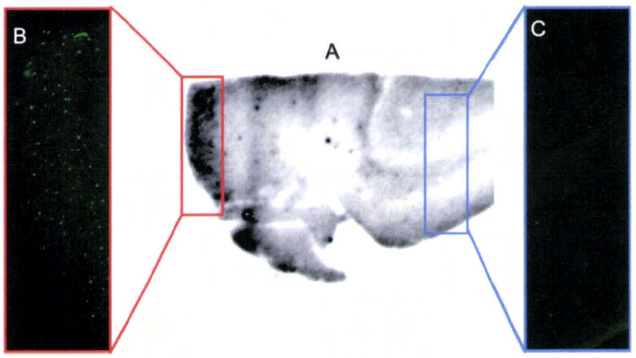

Figure 2. In vitro autoradiography of [^{18}F]**7c** using the human AD brain section (A). Aβ plaques were confirmed by in vitro staining of the same section with thioflavin-S (B and C).

the brain, although a slight difference was observed between the ^{11}C and ^{18}F tracers. When the labeling of plaques in vitro was carried out using sections of brain tissue from an animal model of AD and an AD patient, compound **7c** intensely labeled Aβ plaques existing in both brains. Taken together, the results suggest the novel FPEG chalcone **7c** to be potentially useful for imaging Aβ plaques in the brain using PET.

Experimental Section

General. All reagents were obtained commercially and used without further purification unless otherwise indicated. ^{1}H NMR spectra were obtained on a Varian Gemini 300 spectrometer with TMS as an internal standard. Coupling constants are reported in hertz. Multiplicity was defined by s (singlet), d (doublet), t (triplet) and m (multiplet). Mass spectra were obtained on a JEOL IMS-DX instrument. HPLC analysis was performed on a Shimadzu HPLC system (a LC-10AT pump with a SPD-10A UV detector, $\lambda = 254$ nm) using a Cosmosil C_{18} column (Nakalai Tesque, 5C_{18}-AR-II, 4.6 mm × 150 mm) using acetonitrile/water (50/50) as mobile phase at a flow rate of 1.0 mL/min. All key compounds were proven by this method to show ≥95% purity.

Chemistry. (*E*)-3-(4-(Dimethylamino)phenyl)-1-(4-hydroxyphenyl)-2-propen-1-one (5). 4-Hydroxyacetophenone (1.36 g, 10 mmol) and 4-dimethylaminobenzaldehyde (1.86 g, 10.0 mmol were dissolved in EtOH (15 mL). A 30 mL aliquot of a 10% aqueous KOH solution was then slowly added dropwise to the reaction mixture. The mixture was stirred for 24 h at 100 °C and then extracted with ethyl acetate. After the organic layers were combined and dried over Na_2SO_4, evaporation of the solvent afforded 1.50 g of **5** (84.0%). ^{1}H NMR (CD_3OD) δ: 3.04 (s, 6H), 6.76 (d, $J = 8.7$ Hz, 2H), 6.88 (d, $J = 8.7$ Hz, 2H), 7.50 (d, $J = 15.3$ Hz, 1H), 7.59 (d, $J = 9.0$ Hz, 2H), 7.72 (d, $J = 15.3$ Hz, 1H), 7.98 (d, $J = 8.7$ Hz, 2H). ^{1}H NMR (DMSO-d_6) δ: 2.99 (s, 6H), 6.74 (d, $J = 8.7$ Hz, 2H), 6.88 (d, $J = 8.4$ Hz, 2H), 7.62 (s, 2H), 7.68 (d, $J = 8.7$ Hz, 2H), 8.03 (d, $J = 8.7$ Hz, 2H), 10.30 (s, 1H). EI-MS: m/z 267 (M^+).

(*E*)-3-(4-(Dimethylamino)phenyl)-1-(4-(2-hydroxyethoxy)phenyl)-2-propen-1-one (6a). To a solution of **5** (500 mg, 1.87 mmol and ethylene chlorohydrin (125 μL, 1.87 mmol) in DMSO (5 mL) was added anhydrous K_2CO_3 (775 mg, 5.61 mmol). The reaction mixture was stirred for 18 h at 100 °C and then poured into water and extracted with chloroform. The organic layers were combined and dried over Na_2SO_4. Evaporation of the solvent afforded a residue, which was purified by silica gel chromatography (hexane:ethyl acetate = 1:1) to give 422 mg of **6a** (72.7%). ^{1}H NMR ($CDCl_3$) δ: 3.04 (s, 6H), 4.00−4.01 (m, 2H), 4.17 (t, $J = 4.8$ Hz, 2H), 6.69 (d, $J = 9.0$ Hz, 2H), 6.99 (d, $J = 6.9$ Hz, 2H), 7.35 (d, $J = 15.3$ Hz, 1H), 7.55 (d, $J = 9.0$ Hz, 2H), 7.79 (d, $J = 15.3$ Hz, 1H), 8.02 (d, $J = 9.3$ Hz, 2H).

(*E*)-3-(4-(Dimethylamino)phenyl)-1-(4-(2-(hydroxyethoxy)ethoxy)-phenyl)-2-propen-1-one (6b). The reaction described above to prepare **6a** was used, and **6b** was obtained from **5** and ethylene glycol mono-2-chloroethyl ether. ^{1}H NMR ($CDCl_3$) δ: 3.05 (s, 6H), 3.69 (t, $J = 4.8$ Hz, 2H), 3.78 (s, 2H), 3.91 (t, $J = 4.8$ Hz, 2H), 4.23 (t, $J = 4.8$ Hz, 2H), 6.70 (d, $J = 9.0$ Hz, 2H), 6.99 (d, $J = 9.0$ Hz, 2H), 7.35 (d, $J = 15.3$ Hz, 1H), 7.55 (d, $J = 8.7$ Hz, 2H), 7.79 (d, $J = 15.6$ Hz, 1H), 8.02 (d, $J = 9.0$ Hz, 2H).

(*E*)-3-(4-(Dimethylamino)phenyl)-1-(4-(2-((hydroxyethoxy)ethoxy)-ethoxy)phenyl)-2-propen-1-one (6c). The reaction described above to prepare **6a** was used, and 429 mg of **6c** was obtained in a yield of 82.6% from **5** and 2-[2-(2-chloroethoxy)-ethoxy]ethanol. ^{1}H NMR ($CDCl_3$) δ: 3.04 (s, 6H), 3.62 (t, $J = 5.1$ Hz, 2H), 3.73−3.75 (m, 6H), 3.90 (t, $J = 4.8$ Hz, 2H), 4.22 (t, $J = 4.8$ Hz, 2H), 6.70 (d, $J = 9.0$ Hz, 2H), 6.99 (d, $J = 8.7$ Hz, 2H), 7.35 (d, $J = 15.3$ Hz, 1H), 7.55 (d, $J = 9.0$ Hz, 2H), 7.78 (d, $J = 15.3$ Hz, 1H), 8.02 (d, $J = 9.0$ Hz, 2H).

(*E*)-3-(4-(Dimethylamino)phenyl)-1-(4-(2-fluoroethoxy)phenyl)-2-propen-1-one (7a). To a solution of **6a** (100 mg, 0.32 mmol in 1,2-dimethoxyethane (DME) (5 mL) was added DAST (85 μL, 0.64 mmol) in a dry ice−acetone bath. The reaction mixture was stirred for 1 h at room temperature and then poured into a saturated $NaHSO_3$ solution and extracted with chloroform. After the organic phase was separated, dried over Na_2SO_4, and filtered, and the residue was purified by preparative TLC (hexane:ethyl acetate = 3:1) to give 39 mg of **7a** (38.9%). ^{1}H NMR ($CDCl_3$) δ: 3.09 (s, 6H), 4.30 (d, t, $J_1 = 27.6$ Hz, $J_2 = 4.2$ Hz, 2H), 4.79 (d, t, $J_1 = 47.4$ Hz, $J_2 = 4.2$ Hz, 2H), 6.70 (d, $J = 8.7$ Hz, 2H), 7.00 (d, $J = 9.0$ Hz, 2H), 7.35 (d, $J = 15.6$ Hz, 1H), 7.55 (d, $J = 9.0$ Hz, 2H), 7.79 (d, $J = 15.3$ Hz, 1H), 8.03 (d, $J = 9.0$ Hz, 2H). EI-MS: m/z 313 (M^+).

(*E*)-3-(4-(Dimethylamino)phenyl)-1-(4-(2-(fluoroethoxy)ethoxy)-phenyl)-2-propen-1-one (7b). The reaction described above to prepare **7a** was used, and 28 mg of **7b** was obtained in a yield of 28.0% from **6b**. ^{1}H NMR ($CDCl_3$) δ: 3.04 (s, 6H), 3.77−3.94 (m, 4H), 4.21−4.24 (m, 3H), 4.61 (d, t, $J_1 = 47.4$ Hz, $J_2 = 4.2$ Hz 1H), 6.69 (d, $J = 9.3$ Hz, 2H), 6.99 (d, $J = 8.7$ Hz, 2H), 7.35 (d, $J = 15.3$ Hz, 2H), 7.55 (d, $J = 9.0$ Hz, 2H), 7.78 (d, $J = 15.6$ Hz, 2H), 8.02 (d, $J = 9.0$ Hz, 2H). EI-MS: m/z 357 (M^+).

(*E*)-3-(4-(Dimethylamino)phenyl)-1-(4-(2-((fluoroethoxy)ethoxy)-ethoxy)phenyl)-2-propen-1-one (7c). The reaction described above to prepare **7a** was used, and 29 mg of **7c** was obtained in a yield of 14.4% from **6c** and 2-[2-(2-chloroethoxy)ethoxy]ethanol. ^{1}H NMR ($CDCl_3$) δ: 3.04 (s, 6H), 3.73−3.81 (m, 6H), 3.90 (t, $J = 5.1$ Hz, 2H), 4.21 (t, $J = 5.1$ Hz, 2H), 4.49 (t, $J = 4.5$ Hz, 1H), 4.65 (t, $J = 4.5$ Hz, 1H), 6.70 (d, $J = 8.7$ Hz, 2H), 6.98 (d, $J = 9.0$ Hz, 2H), 7.35 (d, $J = 15.3$ Hz, 1H), 7.55 (d, $J = 8.7$ Hz, 2H), 7.78 (d, $J = 15.3$ Hz, 1H), 8.02 (d, $J = 9.0$ Hz, 2H). EI-MS: m/z 401 (M^+).

1-(4-(2-Hydroxyethoxy)phenyl)ethanone (8a). The reaction described above to prepare **6a** was used, and 1.79 g of **8a** was obtained in a yield of 99.4% from 4-hydroxyacetophenone and ethylene chlorohydrin. ^{1}H NMR ($CDCl_3$) δ: 2.75 (s, 3H), 4.20 (s, 2H), 4.35 (t, $J = 5.1$ Hz, 2H), 7.15 (d, $J = 9.0$ Hz, 2H), 8.13 (d, $J = 9.0$ Hz, 2H).

1-(4-(2-(2-Hydroxyethoxy)ethoxy)phenyl)ethanone (8b). The reaction described above to prepare **6b** was used, and **8b** was obtained from 4-hydroxyacetophenone and ethylene glycol mono-2-chloroethyl ether. ^{1}H NMR ($CDCl_3$) δ: 2.56 (s, 3H), 3.68 (t, $J = 4.8$ Hz 2H), 3.75−3.79 (m, 2H) 3.90 (t, $J = 5.1$ Hz, 2H), 4.21 (t, $J = 4.8$ Hz, 2H), 6.96 (d, $J = 8.7$ Hz, 2H), 7.94 (d, $J = 8.7$ Hz, 2H).

1-(4-(2-(2-(2-Hydroxyethoxy)ethoxy)ethoxy)phenyl)ethanone (8c). The reaction described above to prepare **6a** was used, and **8c** was obtained from 4-hydroxyacetophenone and 2-[2-(chloroethoxy)ethoxy]ethanol. ^{1}H NMR ($CDCl_3$) δ: 2.50 (s, 3H), 3.72−3.83 (m, 6H), 3.92 (t, $J = 4.5$ Hz, 2H), 4.22 (t, $J = 5.1$ Hz, 2H), 4.49 (t, $J = 4.2$ Hz, 1H), 4.61 (t, $J = 4.2$ Hz, 1H), 6.86 (d, $J = 8.7$ Hz, 2H), 7.80 (d, $J = 8.7$ Hz, 2H).

1-(4-(2-Fluoroethoxy)phenyl)ethanone (9a). The reaction described above to prepare **7a** was used, and 1.02 g of **9a** was obtained

in a yield of 63.3% from **8a** and DAST. ^{1}H NMR ($CDCl_3$) δ: 4.24 (d, t, J_1 = 28.2 Hz, J_2 = 4.2 Hz, 2H), 4.75 (d, t, J_1 = 47.1 Hz, J_2 = 3.9 Hz, 2H), 6.92 (d, J = 9.0 Hz, 2H), 7.89 (d, J = 9.3 Hz, 2H).

1-(4-(2-(2-Fluoroethoxy)ethoxy)phenyl)ethanone (9b). The reaction described above to prepare **7b** was used, and **9b** was obtained from **9a** and DAST. ^{1}H NMR ($CDCl_3$) δ: 2.56 (s, 3H), 3.78 (t, J = 3.3 Hz, 1H), 3.86−3.94 (m, 3H), 4.22 (t, J = 5.1 Hz, 2H), 4.51 (t, J = 3.0 Hz, 1H), 4.67 (t, J = 3.0.Hz, 1H), 6.96 (d, J = 8.7 Hz, 2H), 7.93 (d, J = 8.7 Hz, 2H). EI-MS: m/z 226 (M^+).

1-(4-(2-(2-(2-Fluoroethoxy)ethoxy)ethoxy)phenyl)ethanone (9c). The reaction described above to prepare **7c** was used, and 543 mg of **9c** was obtained from **8c** and DAST. ^{1}H NMR ($CDCl_3$) δ: 2.56 (s, 3H), 3.69−3.81 (m, 6H), 3.90 (t, J = 4.5 Hz, 2H), 4.21 (t, J = 5.1 Hz, 2H), 4.49 (t, J = 4.2 Hz, 1H), 4.65 (t, J = 4.2 Hz, 1H), 6.95 (d, J = 9.3 Hz, 2H), 7.92 (d, J = 9.0 Hz, 2H). EI-MS: m/z 270 (M^+).

(*E*)-1-(4-(2-Fluoroethoxy)phenyl)-3-(4-nitrophenyl)-2-propen-1-one (10a). The reaction described above to prepare **5** was used, and 856 mg of **10a** was obtained in a yield of 56.6% from **9a** and 4-nitrobenzaldehyde. ^{1}H NMR ($CDCl_3$) δ: 4.32 (d, t, J_1 = 27.6 Hz, J_2 = 4.2 Hz, 2H), 4.81 (d, t, J_1 = 47.4 Hz, J_2 = 4.2 Hz, 2H), 7.04 (d, J = 8.7 Hz, 2H), 7.65 (d, J = 15.6 Hz, 1H), 7.79 (d, J = 8.7 Hz, 2H), 7.82 (d, J = 12.6 Hz, 1H), 8.06 (d, J = 9.0 Hz, 2H), 8.28 (d, J = 8.7 Hz, 2H).

(*E*)-1-(4-(2-(Fluoroethoxy)ethoxy)phenyl)-3-(4-nitrophenyl)-2-propen-1-one (10b). The reaction described above to prepare **5** was used, and 128 mg of **10b** was obtained from **9b** and 4-nitrobenzaldehyde. ^{1}H NMR ($CDCl_3$) δ: 3.79 (t, J = 4.2 Hz, 1H), 3.88−4.27 (m, 3H), 4.8 (t, J = 4.8 Hz, 2H), 4.53 (t, J = 4.2 Hz, 1H), 4.69 (t, J = 4.2 Hz, 1H), 7.03 (d, J = 8.7 Hz, 2H), 7.66 (d, J = 15.6 Hz, 1H), 7.79 (d, J = 9.0 Hz, 2H), 7.81 (d, J = 15.6 Hz, 1H), 8.05 (d, J = 8.7 Hz, 2H), 8.28 (d, J = 9.0 Hz, 2H).

(*E*)-1-(4-(2-((Fluoroethoxy)ethoxy)ethoxy)phenyl)-3-(4-nitrophenyl)-2-propen-1-one (10c). The reaction described above to prepare **5** was used, and 649 mg of **10c** was obtained from **9c**. ^{1}H NMR ($CDCl_3$) δ: 3.71−3.82 (m, 6H), 3.92 (t, J = 4.5 Hz, 2H), 4.24 (t, J = 4.8 Hz, 2H), 4.50 (t, J = 4.2 Hz, 1H), 4.66 (t, J = 4.5 Hz, 1H), 7.03 (d, J = 9.3 Hz, 2H), 7.66 (d, J = 15.6 Hz, 1H), 7.79 (d, J = 9.0 Hz, 2H), 7.81 (d, J = 15.6 Hz, 1H), 8.05 (d, J = 9.3 Hz, 2H), 8.28 (d, J = 8.7 Hz, 2H).

(*E*)-3-(4-Aminophenyl)-1-(4-(2-fluoroethoxy)phenyl)-2-propen-1-one (11a). A mixture of **10a** (856 mg, 2.7 mmol), $SnCl_2$ (2.55 g, 13.5 mmol), and EtOH (10 mL) was stirred at 100 °C for 2 h. After the mixture had cooled to room temperature, 1 M NaOH (10 mL) was added. The mixture was then extracted with ethyl acetate (10 mL). The organic phase was dried over Na_2SO_4 and filtered. The solvent was removed, and the residue was purified by silica gel chromatography using chloroform as a mobile phase to give 333 mg of **11a** (43.0%). ^{1}H NMR ($CDCl_3$) δ: 4.02 (s, broad, 2H), 4.30 (d, t, J_1 = 27.6 Hz, J_2 = 4.2 Hz, 2H), 4.79 (d, t, J_1 = 47.4 Hz, J_2 = 4.2 Hz, 2H), 6.68 (d, J = 8.7 Hz, 2H), 7.00 (d, J = 8.7 Hz, 2H), 7.36 (d, J = 15.3 Hz, 1H), 7.48 (d, J = 8.4 Hz, 2H), 7.75 (d, J = 15.3 Hz, 1H), 8.03 (d, J = 6.9 Hz, 2H). EI-MS: m/z 285 (M^+).

(*E*)-3-(4-Aminophenyl)-1-(4-(2-(fluoroethoxy)ethoxy)phenyl)-2-propen-1-one (11b). The reaction described above to prepare **11a** was used, and 85 mg of **11b** was obtained from **10b**. ^{1}H NMR ($CDCl_3$) δ: 3.77−3.94 (m, 4H), 4.00 (s, broad, 2H), 4.23 (t, J = 4.5 Hz, 2H), 4.53 (t, J = 4.2 Hz, 1H), 4.69 (t, J = 4.2 Hz, 1H), 6.68 (d, J = 8.4 Hz, 2H), 6.99 (d, J = 8.7 Hz, 2H), 7.74 (d, J = 15.6 Hz, 1H), 7.48 (d, J = 8.4 Hz, 1H), 7.36 (d, J = 15.3 Hz, 1H), 8.01 (d, J = 9.0 Hz, 2H). EI-MS: m/z 329 (M^+).

(*E*)-3-(4-Aminophenyl)-1-(4-(2-((fluoroethoxy)ethoxy)ethoxy)-phenyl)-2-propen-1-one (11c). The reaction described above to prepare **11a** was used, and 206 mg of **11c** was obtained from **10c**. ^{1}H NMR ($CDCl_3$) δ: 3.70−3.83 (m, 6H), 3.89 (t, J = 4.5 Hz, 2H), 4.12 (s, broad, 2H), 4.21 (t, J = 4.8 Hz, 2H), 4.49 (t, J = 4.0 Hz, 1H), 4.65 (t, J = 3.9 Hz, 1H), 6.67 (d, J = 8.7 Hz, 2H), 6.98 (d, J = 8.7 Hz, 2H), 7.36 (d, J = 15.3 Hz, 1H), 7.47 (d, J = 8.4 Hz, 2H), 7.74 (d, J = 15.9 Hz, 1H), 8.01 (d, J = 9.0 Hz, 2H). EI-MS: m/z 373 (M^+).

(*E*)-1-(4-(2-Fluoroethoxy)phenyl)-3-(4-(methylamino)phenyl)-2-propen-1-one (12a). To a solution of **11a** (290 mg, 1.02 mmol) in DMSO (6 mL) were added CH_3I (0.18 mL, 3.05 mmol) and anhydrous K_2CO_3 (691 mg, 5.08 mmol). The reaction mixture was stirred at room temperature for 3 h and poured into water. The mixture was extracted with ethyl acetate. The organic layers were combined and dried over Na_2SO_4. Evaporation of the solvent afforded a residue, which was purified by silica gel chromatography (hexane:ethyl acetate = 2:1) to give 90 mg of **12a** (29.5%). ^{1}H NMR ($CDCl_3$) δ: 2.89 (s, 3H), 4.23 (d, t, J_1 = 27.9 Hz, J_2 = 4.2 Hz, 2H), 4.79 (d, t, J_1 = 47.4 Hz, J_2 = 4.2 Hz, 2H), 6.59 (d, J = 8.7 Hz, 2H), 6.99 (d, J = 9.0 Hz, 2H), 7.34 (d, J = 15.3 Hz, 1H), 7.51 (d, J = 8.4 Hz, 2H), 7.78 (d, J = 15.3 Hz, 1H), 8.02 (d, J = 9.3 Hz, 2H). EI-MS: m/z 299 (M^+).

(*E*)-1-(4-(2-(Fluoroethoxy)ethoxy)phenyl)-3-(4-(methylamino)-phenyl)-2-propen-1-one (12b). The reaction described above to prepare **12a** was used, and 22 mg of **12b** was obtained from **11b**. ^{1}H NMR ($CDCl_3$) δ: 2.90 (s, 3H), 3.78−3.95 (m, 4H), 3.99 (s, broad, 1H), 4.23 (t, J = 4.5 Hz, 2H), 4.53 (t, J = 4.5 Hz, 2H), 4.53 (t, J = 4.2 Hz, 1H), 4.69 (t, J = 4.2 Hz, 1H), 6.60 (d, J = 8.7 Hz, 2H), 6.99 (d, J = 8.7 Hz, 2H), 7.35 (d, J = 15.3 Hz, 1H), 7.51 (d, J = 8.7 Hz, 2H), 7.77 (d, J = 15.3 Hz, 1H), 8.02 (d, J = 8.7 Hz, 2H). EI-MS: m/z 343 (M^+).

(*E*)-1-(4-(2-((Fluoroethoxy)ethoxy)ethoxy)phenyl)-3-(4-(methylamino)phenyl)-2-propen-1-one (12c). The reaction described above to prepare **12a** was used, and 53 mg of **12c** was obtained from **11c**. ^{1}H NMR ($CDCl_3$) δ: 2.89 (s, 3H), 3.69−3.83 (m, 6H), 3.90 (t, J = 4.8 Hz, 2H), 4.12 (s, broad, 1H), 4.22 (t, J = 5.1 Hz, 2H), 4.49 (t, J = 4.2 Hz, 1H), 4.65 (t, J = 4.1 Hz, 1H), 6.60 (d, J = 8.7 Hz, 2H), 6.98 (d, J = 9.0 Hz, 2H), 7.35 (d, J = 15.3 Hz, 1H), 7.51 (d, J = 8.7 Hz, 2H), 7.76 (d, J = 15.3 Hz, 1H), 8.01 (d, J = 8.7 Hz, 2H). EI-MS: m/z 387 (M^+).

(*E*)-3-(4-Dimethylaminophenyl)-1-(4-fluorophenyl)-2-propen-1-one (13). The reaction described above to prepare **5** was used, and 209 mg of **13** was obtained from 4-fluoroacetophenone and 4-dimethylbenzaldehyde. ^{1}H NMR (300 MHz, $CDCl_3$) δ: 3.03 (s, 6H), 6.68 (d, J = 8.7 Hz, 2H), 7.15 (t, J = 8.4 Hz, 2H), 7.30 (d, J = 15.3 Hz, 1H), 7.54 (d, J = 9.0 Hz, 2H), 7.78 (d, J = 15.3 Hz, 1H), 8.02−8.06 (m, 2H). EI-MS: m/z 269 (M^+).

(*E*)-1-(4-Fluorophenyl)-3-(4-nitrophenyl)-2-propen-1-one (14). The reaction described above to prepare **5** was used, and 490 mg of **14** was obtained from 4-fluoroacetophenone and 4-nitrobenzaldehyde. ^{1}H NMR (300 MHz, $CDCl_3$) δ: 7.21 (t, J = 8.7 Hz, 2H), 7.62 (d, J = 15.9 Hz, 1H), 7.80 (d, J = 8.7 Hz, 2H), 7.84 (d, J = 15.9 Hz, 1H), 8.07−8.12 (m, 2H), 8.29 (d, J = 8.7 Hz, 2H). EI-MS: m/z 271 (M^+).

(*E*)-3-(4-Aminophenyl)-1-(4-fluorophenyl)-2-propen-1-one (15). The reaction described above to prepare **11(a−c)** was used, and 150 mg of **15** was obtained from **14**. ^{1}H NMR (300 MHz, $CDCl_3$) δ: 4.07 (s, broad, 2H), 6.67 (d, J = 8.7 Hz, 2H), 7.15 (t, J = 8.7 Hz, 2H), 7.31 (d, J = 15.6 Hz, 1H), 7.47 (d, J = 8.4 Hz, 2H), 7.75 (d, J = 15.6 Hz, 1H), 8.03 (t, J = 8.7 Hz, 2H). EI-MS: m/z 241 (M^+).

(*E*)-1-(4-Fluorophenyl)-3-(4-methylaminophenyl)-2-propen-1-one (16). The reaction described above to prepare **12(a−c)** was used, and 14 mg of **16** was obtained from **15**. ^{1}H NMR (300 MHz, $CDCl_3$) δ: 2.90 (s, 3H), 4.20 (s, broad, 1H), 6.60 (d, J = 8.7 Hz, 2H), 7.17 (d, J = 8.7 Hz, 2H), 7.30 (d, J = 15.6 Hz, 1H), 7.50 (d, J = 8.7 Hz, 2H), 7.78 (d, J = 15.6 Hz, 1H), 8.04 (d, J = 8.7 Hz, 2H). EI-MS: m/z 255 (M^+).

(*E*)-2-(2-(2-(4-(3-(4-(Dimethylamino)phenyl)acryloyl)phenoxy)-ethoxy)ethoxy)ethyl 4-methylbenzenesulfonate (17). To a solution of **6c** (108 mg, 0.27 mmol) in pyridine (3 mL) was added tosyl chloride (343.8 mg, 0.621 mmol). The reaction mixture was stirred for 3 h at room temperature. After water was added, the mixture was extracted with ethyl acetate. The organic layer was dried over Na_2SO_4, and evaporation of the solvent afforded a residue, which was purified by preparative TLC (hexane:ethyl acetate = 1:1) to give 44 mg of **17** (29.4%). ^{1}H NMR (300 MHz, $CDCl_3$) δ: 2.43 (s, 3H), 3.04 (s, 6H), 3.62−3.72 (m, 6H),

3.85−3.87 (m, 2H), 4.15−4.18 (m, 4H), 6.70 (d, J = 8.7 Hz, 2H), 6.98 (d, J = 9.0 Hz, 2H), 7.31−7.35 (m, 2H), 7.37 (d, J = 9.0 Hz, 1H), 7.55 (d, J = 8.7 Hz, 2H), 7.80 (t, J = 8.7 Hz, 3H), 8.02 (d, J = 9.0 Hz, 2H). EI-MS m/z 553 (M^+)

Radiolabeling. Procedure for Labeling of 7a, 7b, 7c, and 13 with ^{11}C. ^{11}C was produced via a ^{14}N(p,α)^{11}C reaction with 16 MeV protons on a target of nitrogen gas with an ultracompact cyclotron (CYPRIS model 325R; Sumitomo Heavy Industry Ltd.) The $^{11}CO_2$ produced was transported to an automated system for the synthesis of ^{11}C-methyl iodide (CUPID C-100; Sumitomo Heavy Industry Ltd.) and converted sequentially to [^{11}C]MeOTf by the previously described method of Jewett.[33] [^{11}C]Chalcones were produced by reacting [^{11}C]MeOTf with the normethyl precursor, **7a**, **7b**, **7c**, and **13**, (0.5 mg) in 500 μL of methyl ethyl ketone (MEK). After the complete transfer of [^{11}C]MeOTf, ^{11}C-methylation was carried out for 5 min and the reaction solvent was then dried with a stream of nitrogen gas. The residue taken up in 200 μL of acetonitrile was purified by a reverse phase HPLC system (a Shimadzu LC-6A isocratic pump, a Shimadzu SPD-6A UV detector, and a Aloka NDW-351D scintillation detector) on a Cosmosil C_{18} column (Nakalai Tesque, 5C_{18}-AR-II, 10 mm × 250 mm) with an isocratic solvent of acetonitrile/water (55/45) at a flow rate of 6.0 mL/min. The desired fraction was collected in a flask and evaporated dry. The radiochemical yield, purity, and specific activity of [^{11}C]chalcones were further confirmed by analytical reverse phase HPLC on a 5C_{18}-AR-300 column (Nakalai Tesque, 4.6 mm × 150 mm, acetonitrile/water (60/40), 1.0 mL/min).

Procedure for Labeling 7c with ^{18}F. [^{18}F]Fluoride was produced by the JSW typeBC3015 cyclotron via an ^{18}O(p,n)^{18}F reaction and passed through a Sep-Pak Light QMA cartridge (Waters) as an aqueous solution in ^{18}O-enriched water. The cartridge was dried by airflow, and the ^{18}F activity was eluted with 0.5 mL of a Kryptofix 222/K_2CO_3 solution (11 mg of Kryptofix 222 and 2.6 mg of K_2CO_3 in acetonitrile/water (86/14)). The solvent was removed at 120 °C under a stream of argon gas. The residue was azeotropically dried with 1 mL of anhydrous acetonitrile twice at 120 °C under a stream of nitrogen gas and dissolved in DMSO (1 mL). A solution of tosylate precursor **17** (1.0 mg) in DMSO (1 mL) was added to the reaction vessel containing the ^{18}F activity in DMSO. The mixture was heated at 160 °C for 5 min. Water (5 mL) was added, and the mixture was passed through a preconditioned Oasis HLB cartridge (3 cm^3) (Waters). The cartridge was washed with 10 mL of water, and the labeled compound was eluted with 2 mL of acetonitrile. The eluted compound was purified by preparative HPLC [YMC-Pack Pro C_{18} column (20 mm × 150 mm), acetonitrile/water (75/25), flow rate 9.0 mL/min]. The retention time of the major byproduct of hydrolysis (t_R = 2.7 min) was well-resolved from the desired ^{18}F-labeled product (t_R = 10.7 min). The radiochemical purity and specific activity were determined by analytical HPLC [YMC-Pack Pro C_{18} column (4.6 mm × 150 mm), acetonitrile/water (60/40), flow rate 1.0 mL/min], and [^{18}F]**7c** was obtained in a radiochemical purity of >99% with the specific activity of 35 GBq/mmol. Specific activity was estimated by comparing the UV peak intensity of the purified ^{18}F-labeled compound with a reference nonradioactive compound of known concentration.

Binding Assays Using the Aggregated Aβ peptides in Solution. Aβ(1−42) was purchased from Peptide Institute (Osaka, Japan). Aggregation was carried out by gently dissolving the peptide (0.25 mg/mL) in a buffer solution (pH 7.4) containing 10 mM sodium phosphate and 1 mM EDTA. The solution was incubated at 37 °C for 42 h with gentle and constant shaking. Binding experiments were carried out as described previously.[18] [^{125}I]DMIC with 2200 Ci/mmol of specific activity and radiochemical purity greater than 95% was prepared using the standard iododestannylation reaction. A mixture containing 50 μL of test compound (0.2 pM-400 μM in 10% EtOH), 50 μL of 0.02 nM [^{125}I]DMIC, 50 μL of Aβ(1−42) aggregates, and 850 μL of 10% EtOH was incubated at room temperature for 3 h. The mixture was then filtered through Whatman GF/B filters using a Brandel M-24 cell harvester, and the radioactivity of the filters containing the bound ^{125}I ligand was measured in a γ counter. Values for the half-maximal inhibitory concentration (IC_{50}) were determined from displacement curves of three independent experiments using GraphPad Prism 4.0, and those for the inhibition constant (K_i) were calculated using the Cheng−Prusoff equation: $K_i = IC_{50}/(1 + [L]/K_d)$, where [L] is the concentration of [^{125}I]DMIC used in the assay and K_d is the dissociation constant of DMIC (4.2 nM).[19] DMIC and IMPY used as test compounds for the inhibition assay were synthesized as reported previously.[19,34]

Biodistribution in Normal Mice. Experiments with animals were conducted in accordance with our institutional guidelines and approved by the Nagasaki University Animal Care Committee and the Kyoto University Animal Care Committee. A 100 μL amount of a saline solution containing the radiolabeled agent (3.7 MBq), EtOH (10%), and ascorbic acid (1 mg/mL) was injected directly into the tail vein of ddY mice (5-week-old, 22−25 g). Groups of five mice were sacrificed at various post-injection time points. The organs of interest were removed and weighed, and the radioactivity was measured with an automatic γ counter (COBRAII, Packard).

Staining of Aβ Plaques in Brain Sections of Tg2576 Transgenic Mice. The Tg2576 transgenic mice (female, 20-month-old) and wild-type (female, 20-month-old) mice were used as an Alzheimer's model and an age-matched control, respectively. After the mice were sacrificed by decapitation, the brains were immediately removed and frozen in powdered dry ice. The frozen blocks were sliced into serial sections 10 μm thick. Each slide was incubated with a 50% EtOH solution (100 μM) of compound **7c** for 10 min. The sections were washed with 50% EtOH for 3 min two times. After drying, the sections were then examined using a microscope (Nikon, Eclipse 80i) equipped with a B-2A filter set (excitation, 450−490 nm; diachronic mirror, 505 nm; long-pass filter, 520 nm). Thereafter, the serial sections were also immunostained with 3,3′-diaminobenzidine (DAB) as a chromogen using monoclonal antibodies against Aβ (amyloid β-protein immunohistostain kit, WAKO).

In Vitro Autoradiography Using Human AD Brains. Postmortem brain tissues from an autopsy-confirmed case of AD (73-year-old male) were obtained from BioChain Institute Inc. The presence and localization of plaques on the sections were confirmed with immunohistochemical staining using a monoclonal Aβ antibody as described above. The sections were incubated with [^{18}F]**7c** (54 μCi/200 μL) for 1 h at room temperature. They were then washed in 50% EtOH (two 1 min wash), before being rinsed with water for 30 s. After drying, the ^{18}F-labeled sections were exposed to a BAS imaging plate (Fuji Film, Tokyo, Japan) for 6 h. Ex vivo autoradiographic images were obtained using a BAS5000 scanner system (Fuji Film). After autoradiographic examination, the same sections were stained by thioflavin-S to confirm the presence of Aβ plaques. For the staining of thioflavin-S, sections were immersed in a 0.125% thioflavin-S solution containing 50% EtOH for 3 min and washed in 50% EtOH. After drying, the sections were then examined using a microscope (Nikon, Eclipse 80i) equipped with a B-2A filter set (excitation, 450−490 nm; diachronic mirror, 505 nm; long-pass filter, 520 nm).

Acknowledgment. This study was supported by the Program for Promotion of Fundamental Studies in Health Sciences of the National Institute of Biomedical Innovation (NIBIO), a Health Labour Sciences Research Grant, and a Grant-in-Aid for Young Scientists (A) and Exploratory Research from the Ministry of Education, Culture, Sports, Science and Technology, Japan.

Supporting Information Available: Representative HPLC chromatograms of [^{18}F]**7c**. This material is available free of charge via the Internet at http://pubs.acs.org.

References

(1) Hardy, J. A.; Higgins, G. A. Alzheimer's disease: the amyloid cascade hypothesis. *Science* **1992**, *256*, 184–185.

(2) Selkoe, D. J. Alzheimer's disease: genes, proteins, and therapy. *Physiol. Rev.* **2001**, *81*, 741–766.

(3) Nordberg, A. PET imaging of amyloid in Alzheimer's disease. *Lancet Neurol.* **2004**, *3*, 519–527.

(4) Mathis, C. A.; Wang, Y.; Klunk, W. E. Imaging β-amyloid plaques and neurofibrillary tangles in the aging human brain. *Curr. Pharm. Des.* **2004**, *10*, 1469–1492.

(5) Klunk, W. E.; Engler, H.; Nordberg, A.; Wang, Y.; Blomqvist, G.; Holt, D. P.; Bergstrom, M.; Savitcheva, I.; Huang, G. F.; Estrada, S.; Ausen, B.; Debnath, M. L.; Barletta, J.; Price, J. C.; Sandell, J.; Lopresti, B. J.; Wall, A.; Koivisto, P.; Antoni, G.; Mathis, C. A.; Langstrom, B. Imaging brain amyloid in Alzheimer's disease with Pittsburgh Compound-B. *Ann. Neurol.* **2004**, *55*, 306–319.

(6) Mathis, C. A.; Wang, Y.; Holt, D. P.; Huang, G. F.; Debnath, M. L.; Klunk, W. E. Synthesis and evaluation of ^{11}C-labeled 6-substituted 2-arylbenzothiazoles as amyloid imaging agents. *J. Med. Chem.* **2003**, *46*, 2740–2754.

(7) Verhoeff, N. P.; Wilson, A. A.; Takeshita, S.; Trop, L.; Hussey, D.; Singh, K.; Kung, H. F.; Kung, M. P.; Houle, S. In vivo imaging of Alzheimer disease β-amyloid with [^{11}C]SB-13 PET. *Am. J. Geriatr. Psychiatry* **2004**, *12*, 584–595.

(8) Ono, M.; Wilson, A.; Nobrega, J.; Westaway, D.; Verhoeff, P.; Zhuang, Z. P.; Kung, M. P.; Kung, H. F. ^{11}C-Labeled stilbene derivatives as Abeta-aggregate-specific PET imaging agents for Alzheimer's disease. *Nucl. Med. Biol.* **2003**, *30*, 565–571.

(9) Small, G. W.; Kepe, V.; Ercoli, L. M.; Siddarth, P.; Bookheimer, S. Y.; Miller, K. J.; Lavretsky, H.; Burggren, A. C.; Cole, G. M.; Vinters, H. V.; Thompson, P. M.; Huang, S. C.; Satyamurthy, N.; Phelps, M. E.; Barrio, J. R. PET of brain amyloid and tau in mild cognitive impairment. *N. Engl. J. Med.* **2006**, *355*, 2652–2663.

(10) Shoghi-Jadid, K.; Small, G. W.; Agdeppa, E. D.; Kepe, V.; Ercoli, L. M.; Siddarth, P.; Read, S.; Satyamurthy, N.; Petric, A.; Huang, S. C.; Barrio, J. R. Localization of neurofibrillary tangles and β-amyloid plaques in the brains of living patients with Alzheimer disease. *Am. J. Geriatr. Psychiatry* **2002**, *10*, 24–35.

(11) Rowe, C. C.; Ackerman, U.; Browne, W.; Mulligan, R.; Pike, K. L.; O'Keefe, G.; Tochon-Danguy, H.; Chan, G.; Berlangieri, S. U.; Jones, G.; Dickinson-Rowe, K. L.; Kung, H. P.; Zhang, W.; Kung, M. P.; Skovronsky, D.; Dyrks, T.; Holl, G.; Krause, S.; Friebe, M.; Lehman, L.; Lindemann, S.; Dinkelborg, L. M.; Masters, C. L.; Villemagne, V. L. Imaging of amyloid β in Alzheimer's disease with ^{18}F-BAY94-9172, a novel PET tracer: proof of mechanism. *Lancet Neurol.* **2008**, *7*, 129–135.

(12) Zhang, W.; Oya, S.; Kung, M. P.; Hou, C.; Maier, D. L.; Kung, H. F. F-18 polyethyleneglycol stilbenes as PET imaging agents targeting Aβ aggregates in the brain. *Nucl. Med. Biol.* **2005**, *32*, 799–809.

(13) Lockhart, A. Imaging Alzheimer's disease pathology: one target, many ligands. *Drug Discovery Today* **2006**, *11*, 1093–1099.

(14) Ye, L.; Morgenstern, J. L.; Gee, A. D.; Hong, G.; Brown, J.; Lockhart, A. Delineation of positron emission tomography imaging agent binding sites on β-amyloid peptide fibrils. *J. Biol. Chem.* **2005**, *280*, 23599–235604.

(15) Lockhart, A.; Ye, L.; Judd, D. B.; Merritt, A. T.; Lowe, P. N.; Morgenstern, J. L.; Hong, G.; Gee, A. D.; Brown, J. Evidence for the presence of three distinct binding sites for the thioflavin T class of Alzheimer's disease PET imaging agents on β-amyloid peptide fibrils. *J. Biol. Chem.* **2005**, *280*, 7677–7684.

(16) Ono, M.; Yoshida, N.; Ishibashi, K.; Haratake, M.; Arano, Y.; Mori, H.; Nakayama, M. Radioiodinated flavones for in vivo imaging of β-amyloid plaques in the brain. *J. Med. Chem.* **2005**, *48*, 7253–7260.

(17) Ono, M.; Watanabe, R.; Kawashima, H.; Kawai, T.; Watanabe, H.; Haratake, M.; Saji, H.; Nakayama, M. ^{18}F-Labeled flavones for in vivo imaging of β-amyloid plaques in Alzheimer's brains. *Bioorg. Med. Chem.* **2009**, *17*, 2069–2076.

(18) Ono, M.; Hori, M.; Haratake, M.; Tomiyama, T.; Mori, H.; Nakayama, M. Structure–activity relationship of chalcones and related derivatives as ligands for detecting of β-amyloid plaques in the brain. *Bioorg. Med. Chem.* **2007**, *15*, 6388–6396.

(19) Ono, M.; Haratake, M.; Mori, H.; Nakayama, M. Novel chalcones as probes for in vivo imaging of β-amyloid plaques in Alzheimer's brains. *Bioorg. Med. Chem.* **2007**, *15*, 6802–6809.

(20) Maya, Y.; Ono, M.; Watanabe, H.; Haratake, M.; Saji, H.; Nakayama, M. Novel radioiodinated aurones as probes for SPECT imaging of β-amyloid plaques in the brain. *Bioconjugate Chem.* **2009**, *20*, 95–101.

(21) Ono, M.; Maya, Y.; Haratake, M.; Ito, K.; Mori, H.; Nakayama, M. Aurones serve as probes of β-amyloid plaques in Alzheimer's disease. *Biochem. Biophys. Res. Commun.* **2007**, *361*, 116–121.

(22) Stephenson, K. A.; Chandra, R.; Zhuang, Z. P.; Hou, C.; Oya, S.; Kung, M. P.; Kung, H. F. Fluoro-pegylated (FPEG) imaging agents targeting Aβ aggregates. *Bioconjugate Chem.* **2007**, *18*, 238–246.

(23) Qu, W.; Kung, M. P.; Hou, C.; Oya, S.; Kung, H. F. Quick assembly of 1,4-diphenyltriazoles as probes targeting β-amyloid aggregates in Alzheimer's disease. *J. Med. Chem.* **2007**, *50*, 3380–3387.

(24) Zhang, W.; Oya, S.; Kung, M. P.; Hou, C.; Maier, D. L.; Kung, H. F. F-18 stilbenes as PET imaging agents for detecting β-amyloid plaques in the brain. *J. Med. Chem.* **2005**, *48*, 5980–5988.

(25) Kung, M. P.; Hou, C.; Zhuang, Z. P.; Zhang, B.; Skovronsky, D.; Trojanowski, J. Q.; Lee, V. M.; Kung, H. F. IMPY: an improved thioflavin-T derivative for in vivo labeling of β-amyloid plaques. *Brain Res.* **2002**, *956*, 202–210.

(26) Hsiao, K.; Chapman, P.; Nilsen, S.; Eckman, C.; Harigaya, Y.; Younkin, S.; Yang, F.; Cole, G. Correlative memory deficits, Aβ elevation, and amyloid plaques in transgenic mice. *Science* **1996**, *274*, 99–102.

(27) Kuntner, C.; Kesner, A. L.; Bauer, M.; Kremslehner, R.; Wanek, T.; Mandler, M.; Karch, R.; Stanek, J.; Wolf, T.; Muller, M.; Langer, O. Limitations of small animal PET imaging with [^{18}F]FDDNP and FDG for quantitative studies in a transgenic mouse model of Alzheimer's disease. *Mol. Imaging Biol.* **2009**, *11*, 236–240.

(28) Klunk, W. E.; Lopresti, B. J.; Ikonomovic, M. D.; Lefterov, I. M.; Koldamova, R. P.; Abrahamson, E. E.; Debnath, M. L.; Holt, D. P.; Huang, G. F.; Shao, L.; DeKosky, S. T.; Price, J. C.; Mathis, C. A. Binding of the positron emission tomography tracer Pittsburgh compound-B reflects the amount of amyloid-β in Alzheimer's disease brain but not in transgenic mouse brain. *J. Neurosci.* **2005**, *25*, 10598–10606.

(29) Maeda, J.; Ji, B.; Irie, T.; Tomiyama, T.; Maruyama, M.; Okauchi, T.; Staufenbiel, M.; Iwata, N.; Ono, M.; Saido, T. C.; Suzuki, K.; Mori, H.; Higuchi, M.; Suhara, T. Longitudinal, quantitative assessment of amyloid, neuroinflammation, and anti-amyloid treatment in a living mouse model of Alzheimer's disease enabled by positron emission tomography. *J. Neurosci.* **2007**, *27*, 10957–10968.

(30) Toyama, H.; Ye, D.; Ichise, M.; Liow, J. S.; Cai, L.; Jacobowitz, D.; Musachio, J. L.; Hong, J.; Crescenzo, M.; Tipre, D.; Lu, J. Q.; Zoghbi, S.; Vines, D. C.; Seidel, J.; Katada, K.; Green, M. V.; Pike, V. W.; Cohen, R. M.; Innis, R. B. PET imaging of brain with the β-amyloid probe, [^{11}C]6-OH-BTA-1, in a transgenic mouse model of Alzheimer's disease. *Eur. J. Nucl. Med. Mol. Imaging* **2005**, *32*, 593–600.

(31) Skovronsky, D. M.; Zhang, B.; Kung, M. P.; Kung, H. F.; Trojanowski, J. Q.; Lee, V. M. In vivo detection of amyloid plaques in a mouse model of Alzheimer's disease. *Proc. Natl. Acad. Sci. U.S.A* **2000**, *97*, 7609–7614.

(32) Saido, T. C.; Iwatsubo, T.; Mann, D. M.; Shimada, H.; Ihara, Y.; Kawashima, S. Dominant and differential deposition of distinct β-amyloid peptide species, Aβ N3(pE), in senile plaques. *Neuron* **1995**, *14*, 457–466.

(33) Jewett, D. M. A simple synthesis of [^{11}C]methyl triflate. *Int. J. Radiat. Appl. Instrum. A* **1992**, *43*, 1383–1385.

(34) Zhuang, Z. P.; Kung, M. P.; Wilson, A.; Lee, C. W.; Plossl, K.; Hou, C.; Holtzman, D. M.; Kung, H. F. Structure–activity relationship of imidazo[1,2-*a*]pyridines as ligands for detecting β-amyloid plaques in the brain. *J. Med. Chem.* **2003**, *46*, 237–243.

Bioorganic & Medicinal Chemistry 17 (2009) 7002–7007

Contents lists available at ScienceDirect

Bioorganic & Medicinal Chemistry

journal homepage: www.elsevier.com/locate/bmc

Push–pull benzothiazole derivatives as probes for detecting β-amyloid plaques in Alzheimer's brains

Masahiro Ono [a,*,†], Shun Hayashi [a,†], Hiroyuki Kimura [a], Hidekazu Kawashima [b], Morio Nakayama [c], Hideo Saji [a,*]

[a] Graduate School of Pharmaceutical Sciences, Kyoto University, 46-29 Yoshida Shimoadachi-cho, Sakyo-ku, Kyoto 606-8501, Japan
[b] Graduate School of Medicine, Kyoto University, Shogoin Kawahara-cho, Kyoto 606-8507, Japan
[c] Graduate School of Biomedical Sciences, Nagasaki University, 1-14 Bunkyo-machi, Nagasaki 852-8521, Japan

ARTICLE INFO

Article history:
Received 29 June 2009
Revised 4 August 2009
Accepted 4 August 2009
Available online 20 August 2009

Keywords:
β-Amyloid
Push–pull dye
Imaging
Alzheimer's disease

ABSTRACT

We synthesized push–pull benzothiazole derivatives and evaluated their potential as β-amyloid imaging probes. In binding experiments in vitro, the benzothiazoles showed excellent affinity for synthetic Aβ(1-42) aggregates. β-Amyloid plaques in the mouse and human brain were clearly visualized with the benzothiazoles, reflecting the results in vitro. These compounds may be a useful scaffold for the development of novel PET/SPECT and fluorescent tracers for detecting β-amyloid in Alzheimer's brains.

1. Introduction

The formation of β-amyloid (Aβ) plaques is a key neurodegenerative event in Alzheimer's disease (AD).[1,2] Since the imaging of these plaques in vivo may lead to the presymptomatic diagnosis of AD, many molecular probes for this purpose, including PET/SPECT and MRI tracers, have been developed.[3–12] The PET ligand [^{11}C]-2-(4-(methylamino)phenyl)-6-hydroxybenzothiazole (6-OH-BTA-1 or PIB) with a benzothiazole backbone (Fig. 1) has shown particular promise in early clinical trials and is currently being used in a number of human studies.[13–15] In addition to PET/SPECT and MRI probes, much attention has focused on the development of near-infrared fluorescent (NIRF) probes targeting Aβ plaques.[16–18] NIRF probes are typically small molecule fluorescent dyes designed to absorb and emit light in the near-infrared region, where tissue scattering and absorption is lowest. The simple synthesis, low-cost, and long shelf-life of NIRF probes, together with the low-cost of optical imaging devices, present an attractive alternative to MRI and PET/SPECT techniques.

Among NIRF probes reported, to date, NIAD crosses the blood–brain barrier, selectively binds Aβ with high affinity, clears quickly from the brain, and absorbs and emits within the near-infrared region (650–900 nm), often called the 'optical window' (Fig. 1).[17] A series of NIAD derivatives have been designed and synthesized based on a classical push–pull architecture with terminal donor (hydroxy or dimethylamino group) and acceptor (dicyanomethylene group) moieties that are interconnected by a highly polarized bridge (dithienylethenyl group), because various donor and acceptor groups can be used to manipulate the relative energies of HOMO and LUMO and obtain the desired long wavelength of absorption/emission bands.[17]

On the basis of this approach to the molecular design, we planned to develop novel push–pull dyes for detecting Aβ plaques in the brain. We selected benzothiazole or styrylbenzothiazole as the highly polarized bridge, a dimethylamino group as the donor, and a dicyanomethylene group as the acceptor. In the present study, we designed and synthesized two benzothiazole-derived push–pull dyes (PP-BTA-1 and PP-BTA-2 in Fig. 2), and evaluated their biological potential as probes for detecting Aβ plaques in the brain. To our knowledge, this is the first time push–pull benzothiazole derivatives have been proposed as Aβ imaging probes for detecting AD.

2. Results and discussion

The target benzothiazole derivatives were prepared as shown in Schemes 1 and 2. PP-BTA-1 (**4**) was successfully synthesized in a yield of 21.4% according to methods reported previously (Scheme

* Corresponding authors. Tel.: +81 75 753 4608; fax: +81 75 753 4568 (M.O), tel.: +81 75 753 4556; fax: +81 75 753 4568 (H.S.).
E-mail addresses: ono@pharm.kyoto-u.ac.jp (M. Ono), hsaji@pharm.kyoto-u.ac.jp (H. Saji).
† These authors contributed equally to this work.

0968-0896/$ - see front matter © 2009 Elsevier Ltd. All rights reserved.
doi:10.1016/j.bmc.2009.08.032

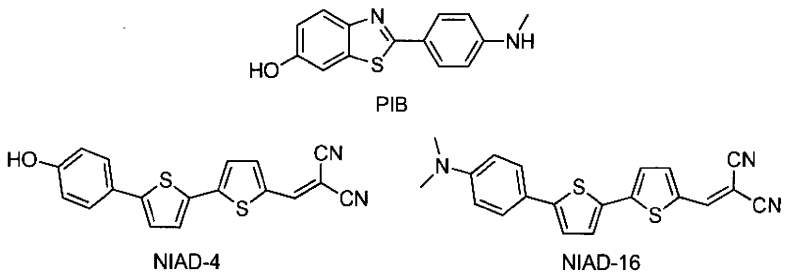

Figure 1. Chemical structures of PIB, NIAD-4 and NIAD-16.

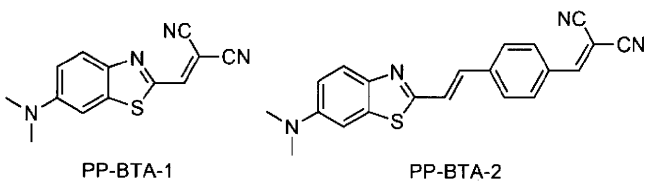

Figure 2. Chemical structures of push–pull benzothiazole derivatives reported in this paper.

1).[19] The formation of styrylbenzothiazole in the synthesis of PP-BTA-2 (**7**) (Scheme 2) was achieved by a Wadsworth–Emmons reaction between diethyl (4-cyanobenzyl)phosphonate and 6-dimethylaminobenzothiazole-2-carbaldehyde. The desired (*E*)-styrylbenzothiazole derivative was prepared in a yield of 23.0%. The cyano group was converted to a formyl group by a reaction with DIBAL-H as reported.[20] The target PP-BTA-2 was prepared by the condensation of carbaldehyde with malononitrile.

NIRF imaging in vivo requires the development of new fluorescent compounds with optimal fluorescent properties and high affinity for Aβ plaques. First, we evaluated the fluorescent properties (absorption/emission wavelengths) of PP-BTA-1 and PP-BTA-2. PP-BTA-1 and PP-BTA-2 exhibited absorption/emission peaks at 540/634 nm and 410/529 nm in EtOH, respectively. The extension of π-conjugation generally leads to absorption/emission bands with longer wavelengths. However, PP-BTA-2 showed a shorter wavelength than PP-BTA-1 despite a longer π-conjugation. On the other hand, because the wavelength of PP-BTA-1 is close to the near-infrared region, a slight modification should lead to a wavelength appropriate for imaging in vivo. Furthermore, when PP-BTA-1 and PP-BTA-2 existed in a solution containing Aβ(1-42) aggregates, the fluorescence intensity of PP-BTA-1 and PP-BTA-2 increased with the concentration of Aβ(1-42) aggregates, indicating affinity for Aβ aggregates (Fig. 3).

To quantify the affinity of push–pull benzothiazole derivatives for Aβ plaques, we carried out inhibition assays on the binding to Aβ(1-42) aggregates with thioflavin T as a competing ligand. PP-BTA-1 and PP-BTA-2 displaced thioflavin T in a dose-dependent manner, indicating that they have affinity for Aβ(1-42) aggregates (Fig. 4). In addition, this result suggests that PP-BTA-1 and PP-BTA-2 may occupy a binding site on Aβ aggregates similar to that of thioflavin T. The apparent IC_{50} values for PP-BTA-1, PP-BTA-2 and PIB were 0.12, 0.11 and 0.67 μM, respectively (Table 1). The IC_{50} of

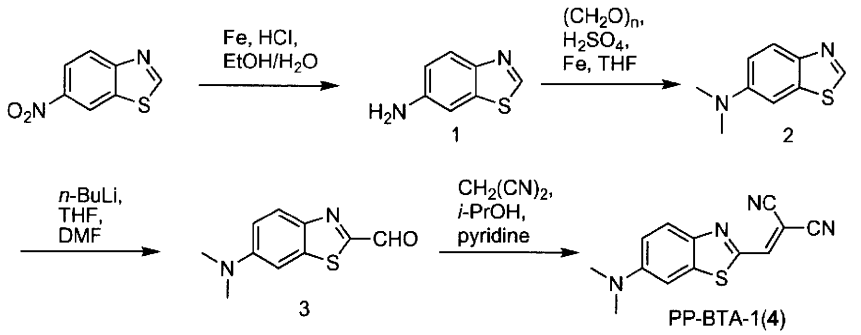

Scheme 1.

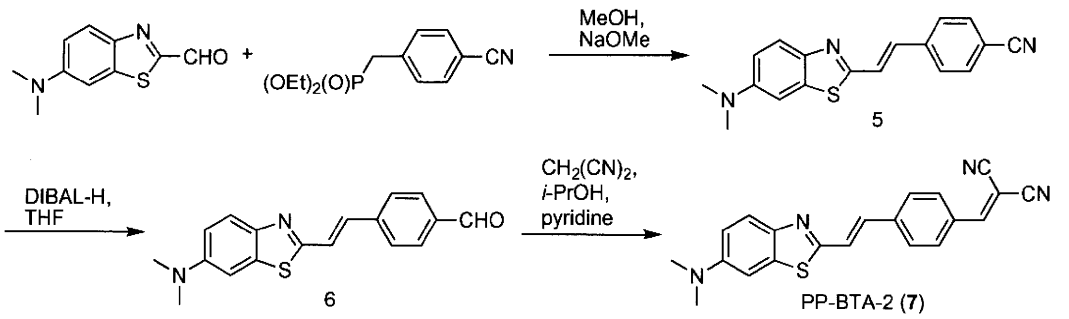

Scheme 2.

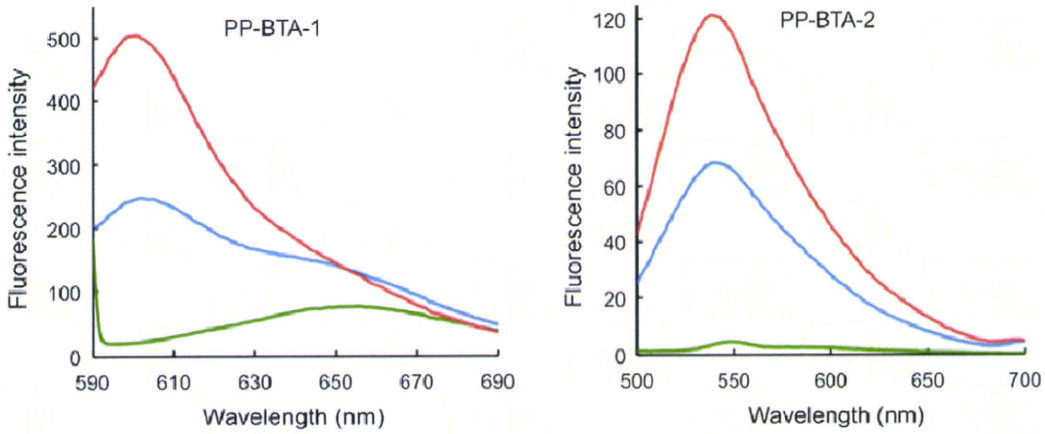

Figure 3. Aβ-dependent change in the fluorescence spectra of PP-BTA-1 and PP-BTA-2. Green, blue and red lines show the fluorescence spectrum of 0, 5 and 10 μg/mL of Aβ(1-42) aggregates, respectively.

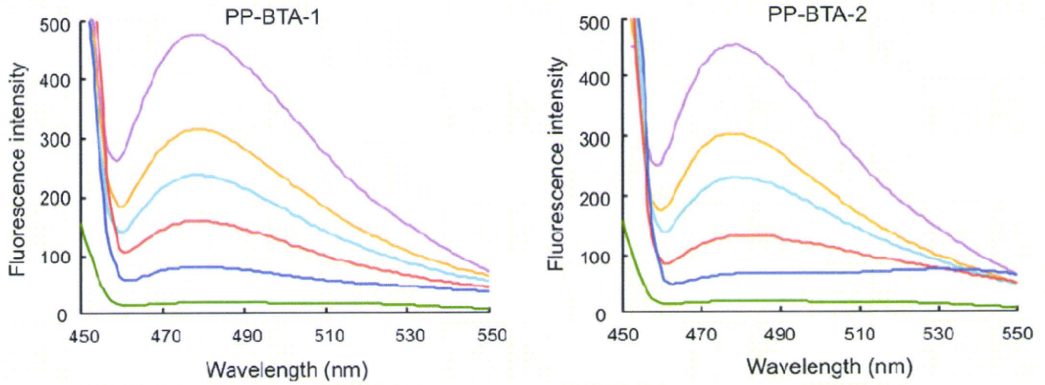

Figure 4. Inhibition assays of PP-BTA-1 and PP-BTA-2 using thioflavin T as the ligand in Aβ(1-42) aggregates. Fluorescence spectral change of thioflavin T (3 μM) upon addition of 0.0611 (orange line), 0.122 (cyan line), 0.486 (red line), or 2.65 (blue line) μM of PP-BTA-1 and PP-BTA-2 to Aβ(1-42) aggregates (10 μg/mL). A pink line shows the fluorescence spectrum of thioflavin T (3 μM) with Aβ(1-42) aggregates. A green line shows the fluorescence spectrum of thioflavin T (3 μM) alone.

Table 1
Apparent inhibition constants (IC_{50}, μM) of benzothiazoles for the binding of thioflavin T to Aβ(1-42) aggregates

Compound	IC_{50}[a] (μM)
PP-BTA-1 (**4**)	0.12 ± 0.001
PP-BTA-2 (**7**)	0.11 ± 0.001
PIB	0.67 ± 0.11

[a] Each value represents the mean ± standard error of the mean for three independent experiments.

PP-BTA-1 and PP-BTA-2 was lower than that of PIB, which is commonly used for clinical research, indicating PP-BTA-1 and PP-BTA-2 to have greater affinity for Aβ(1-42) aggregates. While PP-BTA-1 does not have the phenyl group in the phenylbenzothiazole structure that PIB possesses, it showed stronger binding to Aβ aggregates than PIB. Moreover, benzothiazole is a compact molecule advantageous for penetration of the blood–brain barrier after administration in vivo. These results suggest benzothiazole to be a useful scaffold for the development of Aβ imaging agents in vivo.

Next, the usefulness of PP-BTA-1 and PP-BTA-2 for neuropathological staining of Aβ plaques was investigated in an animal model of AD, the Tg2576 mouse, specifically engineered to overproduce Aβ plaques in the brain. PP-BTA-1 and PP-BTA-2 clearly stained the plaques as reflected by the high affinity for Aβ aggregates in in vitro competition assays (Fig. 5). The labeling pattern was consistent with that observed with thioflavin S. In contrast, wild-type mice displayed no remarkable accumulation of PP-BTA-1 and PP-BTA-2 in brain sections. These results suggest that PP-BTA-1 and PP-BTA-2 show affinity for Aβ plaques in the mouse brain in addition to having affinity for synthetic Aβ(1-42) aggregates.

Furthermore, we also investigated the effectiveness of PP-BTA-1 and PP-BTA-2 for neuropathological staining of Aβ plaques in human AD brain sections (Fig. 6). A previous report suggested the configuration/folding of Aβ plaques in Tg2576 mice to be different from the tertiary/quaternary structure of Aβ plaques in AD brains.[21] Therefore, it is important to evaluate the binding affinity for Aβ plaques in human AD brains. PP-BTA-1 and PP-BTA-2 clearly stained many neuritic plaques in AD brains (Fig. 6A and D). In contrast, no apparent staining was observed in adult normal brain sections (Fig. 6C and F). The labeling pattern was consistent with that observed by immunohistochemical labeling with an antibody specific to Aβ Fig. 6B and E), indicating that PP-BTA-1 and PP-BTA-2 may be applicable for in vivo imaging of Aβ plaques in Alzheimer's brains and deserve further investigation as a potential tool for early diagnosis.

Since PP-BTA-1 and PP-BTA-2 possess a dimethylamino group, they can be used as probes for PET by labeling one of two methyl groups with $^{11}CH_3$. In addition, for the application of push–pull benzothiazole derivatives to optical imaging in vivo, the fine-tuning of absorption/emission wavelengths to a desired region continues by optimizing the combination of donor and acceptor groups.

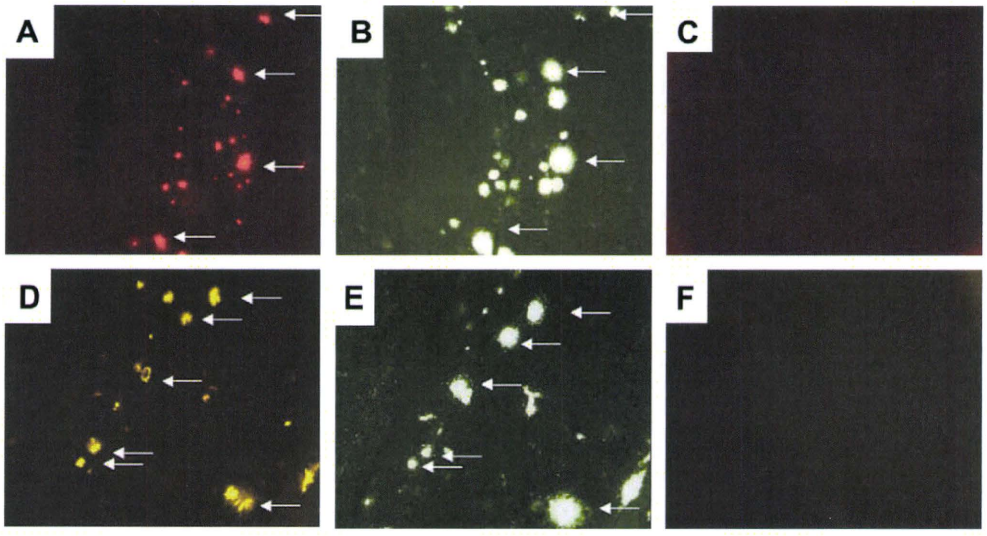

Figure 5. Neuropathological staining of PP-BTA-1 and PP-BTA-2 in 10 μm sections from a mouse model of AD (A and D) and a wild-type mouse (C and F). Aβ plaques labeled with PP-BTA-1 and PP-BTA-2 were confirmed by staining of the serial sections using thioflavin S (B and E).

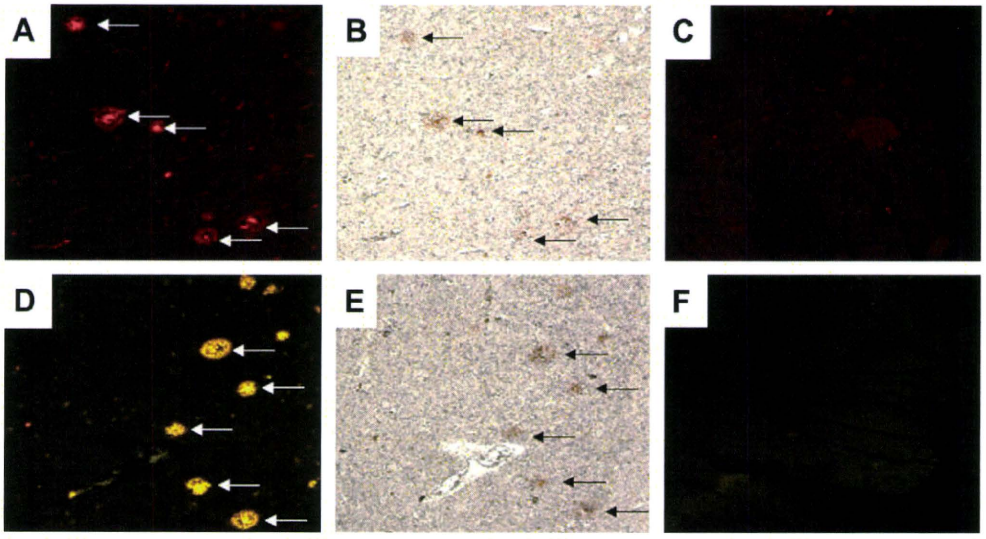

Figure 6. Neuropathological staining of 5 μm AD brain sections from the temporal cortex (A, B, D and E) and adult normal temporal brain sections (C and F). Many neuritic plaques are clearly stained with PP-BTA-1 (A) and PP-BTA-2 (D). Intense fluorescence can be seen in the core of neuritic plaques. Aβ immunostaining with anti Aβ antibodies in the serial sections shows an identical staining pattern of plaques (B and E). No apparent staining was observed in adult normal brain sections (C and F).

3. Conclusion

In conclusion, we successfully designed and synthesized benzothiazole-derived push–pull dyes for imaging Aβ plaques in the brain. In binding experiments in vitro, these benzothiazole compounds showed high affinity for Aβ(1-42) aggregates. PP-BTA-1 and PP-BTA-2 clearly stained Aβ plaques in both mouse brain and human brain, reflecting their affinity for Aβ aggregates in vitro. These findings suggest that additional structural changes on the benzothiazole backbone may be applied to potential Aβ probes for not only optical imaging but also PET and SPECT.

4. Experimental

^{1}H NMR spectra were obtained on a JEOL JNM-LM400 with TMS as an internal standard. Coupling constants are reported in hertz. Multiplicity was defined by s (singlet), d (doublet), t (triplet), br (broad) and m (multiplet). Mass spectra were obtained on a SHIMADZU LCMS-2010 EV. PIB was purchased from ABX (Radeberg, Germany). Other reagents were of reagent grade and used without further purification unless otherwise indicated.

4.1. Chemistry

4.1.1. 1,3-Benzothiazol-6-amine (1)

To a mixture of 6-nitrobenzothiazole (2.5 g, 13.9 mmol) and concentrated HCl (1.93 mL, 22.7 mmol) in 80% EtOH (63 mL) was added powdered iron (3.7 g, 55.6 mmol). The reaction mixture was stirred for 1 h under reflux, and then cooled to room temperature. The precipitate of iron oxides and hydroxy salts was removed by filtration. The solvent was removed and the solid residue was extracted into a heterogeneous mixture of EtOAc (50 mL × 2) and a 10% aqueous solution of Na_2CO_3 (50 mL). The EtOAc extract was dried (Na_2SO_4) and the solvent was removed under vacuum to yield **1** (1.91 g, 91.7%). ^{1}H NMR (400 MHz, $CDCl_3$) δ 8.70 (s, 1H), 7.89 (d, J = 8.8 Hz, 1H), 7.17 (d, J = 2.4 Hz, 1H), 6.87 (dd, J = 8.8, 2.4 Hz, 1H), 3.85 (br s, 2H). MS m/z 151 [MH^+].

4.1.2. *N,N*-Dimethyl-1,3-benzothiazol-6-amine (2)

A solution of **1** (1.47 g, 9.8 mmol) in THF (40 mL) was slowly added to a stirred mixture of 40% aqueous formaldehyde (7.24 mL, 98 mmol) and 4 M H_2SO_4 (7.95 mL, 29.4 mL). Powdered iron (4.36 g, 78.4 mL) was then added and the mixture was vigorously stirred for 3 h. The precipitate of iron salts was removed by filtration and washed with EtOAc (20 mL × 2). The combined organic solutions were made strongly basic with 1 N NaOH (50 mL) and extracted with EtOAc (50 mL × 2). The combined EtOAc extracts were dried (Na_2SO_4) and the solvent was removed on a rotary vacuum evaporator. The oily residue was purified by silica gel chromatography (hexane/EtOAc = 4:1) to give **2** (460 mg, 26.3%). ^{1}H NMR (400 MHz, $CDCl_3$) δ 8.67 (s, 1H), 7.95 (d, J = 8.8 Hz, 1H), 7.15 (d, J = 2.4 Hz, 1H), 7.00 (dd, J = 8.8, 2.4 Hz, 1H), 3.04 (s, 6H). MS m/z 179 [MH^+].

4.1.3. 6-(Dimethylamino)-1,3-benzothiazole-2-carbaldehyde (3)

To a vigorously stirred solution of *n*-BuLi (0.5 mL, 2.6 M in hexane, 1.3 mmol) in THF (5.8 mL) at −78 °C under N_2 was added slowly a solution of **2** (220 mg, 1.23 mmol). The reaction mixture was stirred, warmed to −50 °C and after 1 h cooled to −78 °C. To the resulting solution of aryllithium salt was added slowly anhydrous DMF (0.38 mL). The solution was stirred for 2 h, poured into H_2O (9 mL), neutralized with an aqueous saturated solution of NH_4Cl and subsequently extracted with EtOAc (20 mL × 2). The combined extracts were dried over Na_2SO_4 and the solvent was removed under vacuum to give **3** (255 mg, 97.3%). ^{1}H NMR (400 MHz, $CDCl_3$) δ 10.06 (s, 1H), 8.03 (d, J = 10.0 Hz, 1H), 7.07–7.04 (m, 2H), 3.12 (s, 6H). MS m/z 207 [MH^+].

4.1.4. ((6-(Dimethylamino)-1,3-benzothiazol-2-yl)methylene)-malononitrile (PP-BTA-1, 4)

A solution of **3** (124 mg, 0.6 mmol), malononitrile (60 mg, 0.9 mmol) and pyridine (0.12 mL) in 2-propanol (7.2 mL) was stirred and refluxed for 30 min. The mixture was poured into H_2O (20 mL) and extracted with $CHCl_3$ (20 mL × 3). The combined extracts were dried over Na_2SO_4 and the solvent was removed under vacuum to give **4** (152 mg, 91.7%). ^{1}H NMR (400 MHz, $CDCl_3$) δ 7.99 (s, 1H), 7.99 (d, J = 9.2 Hz, 1H), 7.08 (dd, J = 9.2, 2.4 Hz, 1H), 7.02 (d, J = 2.4 Hz, 1H), 3.16 (s, 6H). MS m/z 255 [MH^+]. Anal. Calcd for $C_{13}H_{10}N_4S$: C, 61.40; H, 3.96; N, 22.03; S, 12.61. Found: C, 61.34; H, 3.84; N, 21.82; S, 12.64.

4.1.5. 4-((*E*)-2-(6-(Dimethylamino)-1,3-benzothiazol-2-yl) vinyl)benzonitrile (5)

To a solution of (4-cyanobenzyl)phosphonate (403.6 mg, 1.6 mmol) in MeOH (12.8 mL) was added NaOMe (0.632 mL). The mixture was cooled in an ice bath, and stirred under reflux for 3 h after the addition of **3** (330 mg, 1.6 mmol). The solid that formed in the reaction mixture was filtered to give **5** (385 mg, 78.8%). ^{1}H NMR (400 MHz, $CDCl_3$) δ 7.84 (d, J = 9.6 Hz, 1H), 7.64 (dd, J = 21.2, 8.0 Hz, 4H), 7.45 (d, J = 16.4 Hz, 1H), 7.32 (d, J = 16.4 Hz, 1H), 7.06 (d, J = 2.8 Hz, 1H), 6.95 (dd, J = 9.6, 2.8 Hz, 1H), 3.06 (s, 6H). MS m/z 306 [MH^+].

4.1.6. 4-((*E*)-2-(6-(Dimethylamino)-1,3-benzothiazol-2-yl) vinyl)benzaldehyde (6)

To a solution of **5** (61 mg, 0.2 mmol) in THF (3.3 mL) was added DIBAL-H (1 M in hexane, 0.5 mL) at −78 °C. The reaction mixture was stirred at room temperature overnight. Thereafter, 10% acetic acid (15 mL) was added and the mixture was extracted with $CHCl_3$ (20 mL × 2). After the organic layer was washed with saline, the combined extracts were dried over Na_2SO_4. The residue was purified by silica gel chromatography (hexane/EtOAc = 2:1) to give **6** (28 mg, 45.4%). ^{1}H NMR (400 MHz, $CDCl_3$) δ 10.02 (s, 1H), 7.90 (d, J = 8.4 Hz, 2H), 7.85 (d, J = 8.2 Hz, 1H), 7.67 (d, J = 8.4 Hz, 2H), 7.50 (d, J = 16.4 Hz, 1H), 7.38 (d, J = 16.4 Hz, 1H), 7.07 (d, J = 2.4 Hz, 1H), 6.96 (dd, J = 8.8, 2.4 Hz, 1H), 3.06 (s, 6H). MS m/z 309 [MH^+].

4.1.7. 4-((*E*)-2-(6-(Dimethylamino)-1,3-benzothiazol-2-yl) vinyl)benzylidene)malononitrile (PP-BTA-2, 7)

The same reaction as described above to prepare **5** was used, and 45 mg of **7** was obtained in a 63.5% yield from **6**. ^{1}H NMR (400 MHz, $CDCl_3$) δ 7.94 (d, J = 8.4 Hz, 2H), 7.86 (d, J = 8.8 Hz, 1H), 7.73 (s, 1H), 7.68 (d, J = 8.4 Hz, 2H), 7.53 (d, J = 16.4 Hz, 1H), 7.35 (d, J = 16.4 Hz, 1H), 7.08 (s, 1H), 6.97 (d, J = 10.0 Hz , 1H), 3.08 (s, 6H). MS m/z 357 [MH^+]. Anal. Calcd for $C_{21}H_{16}N_4S$: C, 70.76; H, 4.52; N, 15.72; S, 9.00. Found: C, 70.48; H, 4.57; N, 15.43; S, 8.99.

4.2. Fluorescence experiments

PP-BTA-1 and PP-BTA-2 were dissolved in 5% EtOH at 10 μM. The fluorescence of PP-BTA-1 and PP-BTA-2 was measured with a spectrophotometer (RF-1500, Shimadzu, Japan). For some measurements, the spectra of PP-BTA-1 and PP-BTA-2 were determined with or without Aβ(1-42) aggregates (0, 5 and 10 μM).

4.3. Binding experiments using Aβ(1-42) aggregates

A solid form of Aβ(1-42) was purchased from Peptide Institute (Osaka, Japan). Aggregation was carried out by gently dissolving the peptide (0.25 mg/mL) in a buffer solution (pH 7.4) containing 10 mM sodium phosphate and 1 mM EDTA. The solution was incubated at 37 °C for 42 h with gentle and constant shaking. Thioflavin-T was used as the tracer for the competition binding experiments. A mixture (3.6 mL of 10% EtOH) containing PP-BTA-1, PP-BTA-2 and PIB (final concn 61.1 nM–5.48 μM), thioflavin-T (final concn 3 μM), and Aβ(1-42) aggregates (final concn 10 μg/mL) was incubated at room temperature for 10 min. Fluorescence intensity at an excitation wavelength of 445 nm was plotted, and values for the apparent half-maximal inhibitory concentration (IC_{50}) were determined from a calibration curve of fluorescence intensity at 478 nm in three independent experiments.

4.4. Staining of Aβ plaques in Tg2576 mouse brain sections

The experiments with animals were conducted in accordance with our institutional guidelines and approved by the Kyoto University Animal Care Committee. The Tg2576 transgenic mice (female, 27-month-old) and wild-type mice (female, 27-month-old) were used as the Alzheimer's model and control mice, respectively. After the mice were sacrificed by decapitation, the brains were immediately removed and frozen in powdered dry ice. The frozen blocks were sliced into serial sections, 10 μm thick. Each slide was incubated with a 50% EtOH solution (100 μM) of PP-BTA-1 and PP-BTA-2 for 10 min. The sections were washed in 50% EtOH for 1 min two times, and examined using a microscope (Nikon Eclipse 80i) equipped with a G-2A filter set (excitation, 510–560 nm; diachronic mirror, 575 nm; longpass filter, 470 nm) for PP-BTA-1, and a B-2A filter set (excitation, 450–480 nm; diachronic mirror, 505 nm; longpass filter, 520 nm) for PP-BTA-2. Thereafter, the serial sections were also stained with thioflavin S, a pathological dye commonly used for staining Aβ plaques in the brain, and examined using a microscope (Nikon Eclipse 80i) equipped with a BV-2A filter set (excitation, 400–440 nm; diachronic mirror, 455 nm; longpass filter, 470 nm).

4.5. Staining of Aβ plaques in human AD brain sections

Postmortem brain tissues from an autopsy-confirmed case of AD (73-year-old male) and a control subject (36-year-old male) were

obtained from BioChain Institute Inc. The sections were incubated with PP-BTA-1 and PP-BTA-2 (50% EtOH, 100 μM) for 10 min at room temperature. The sections were washed in 50% EtOH for 1 min two times, and examined using a microscope (Nikon Eclipse 80i) equipped with a G-2A filter set (excitation, 510–560 nm; diachronic mirror, 575 nm; longpass filter, 470 nm) for PP-BTA-1, and a B-2A filter set (excitation, 450–480 nm; diachronic mirror, 505 nm; longpass filter, 520 nm) for PP-BTA-2. The presence and localization of plaques on the same sections were confirmed with immunohistochemical staining using a monoclonal Aβ antibody, BC05 (Wako).

Acknowledgements

This study was supported by the Program for Promotion of Fundamental Studies in Health Sciences of the National Institute of Biomedical Innovation (NIBIO), a Health Labour Sciences Research Grant, and a Grant-in-Aid for Young Scientists (A) and Exploratory Research from the Ministry of Education, Culture, Sports, Science and Technology, Japan.

References and notes

1. Klunk, W. E. *Neurobiol. Aging* **1998**, *19*, 145.
2. Selkoe, D. J. *Physiol. Rev.* **2001**, *81*, 741.
3. Shoghi-Jadid, K.; Small, G. W.; Agdeppa, E. D.; Kepe, V.; Ercoli, L. M.; Siddarth, P.; Read, S.; Satyamurthy, N.; Petric, A.; Huang, S. C.; Barrio, J. R. *Am. J. Geriatr. Psychiat.* **2002**, *10*, 24.
4. Mathis, C. A.; Wang, Y.; Holt, D. P.; Huang, G. F.; Debnath, M. L.; Klunk, W. E. *J. Med. Chem.* **2003**, *46*, 2740.
5. Ono, M.; Wilson, A.; Nobrega, J.; Westaway, D.; Verhoeff, P.; Zhuang, Z. P.; Kung, M. P.; Kung, H. F. *Nucl. Med. Biol.* **2003**, *30*, 565.
6. Klunk, W. E.; Engler, H.; Nordberg, A.; Wang, Y.; Blomqvist, G.; Holt, D. P.; Bergstrom, M.; Savitcheva, I.; Huang, G. F.; Estrada, S.; Ausen, B.; Debnath, M. L.; Barletta, J.; Price, J. C.; Sandell, J.; Lopresti, B. J.; Wall, A.; Koivisto, P.; Antoni, G.; Mathis, C. A.; Langstrom, B. *Ann. Neurol.* **2004**, *55*, 306.
7. Verhoeff, N. P.; Wilson, A. A.; Takeshita, S.; Trop, L.; Hussey, D.; Singh, K.; Kung, H. F.; Kung, M. P.; Houle, S. *Am. J. Geriatr. Psychiat.* **2004**, *12*, 584.
8. Small, G. W.; Kepe, V.; Ercoli, L. M.; Siddarth, P.; Bookheimer, S. Y.; Miller, K. J.; Lavretsky, H.; Burggren, A. C.; Cole, G. M.; Vinters, H. V.; Thompson, P. M.; Huang, S. C.; Satyamurthy, N.; Phelps, M. E.; Barrio, J. R. *N. Eng. J. Med.* **2006**, *355*, 2652.
9. Kudo, Y.; Okamura, N.; Furumoto, S.; Tashiro, M.; Furukawa, K.; Maruyama, M.; Itoh, M.; Iwata, R.; Yanai, K.; Arai, H. *J. Nucl. Med.* **2007**, *48*, 553.
10. Rowe, C. C.; Ackerman, U.; Browne, W.; Mulligan, R.; Pike, K. L.; O'Keefe, G.; Tochon-Danguy, H.; Chan, G.; Berlangieri, S. U.; Jones, G.; Dickinson-Rowe, K. L.; Kung, H. P.; Zhang, W.; Kung, M. P.; Skovronsky, D.; Dyrks, T.; Holl, G.; Krause, S.; Friebe, M.; Lehman, L.; Lindemann, S.; Dinkelborg, L. M.; Masters, C. L.; Villemagne, V. L. *Lancet. Neurol.* **2008**, *7*, 129.
11. Higuchi, M.; Iwata, N.; Matsuba, Y.; Sato, K.; Sasamoto, K.; Saido, T. C. *Nat. Neurosci.* **2005**, *8*, 527.
12. Poduslo, J. F.; Curran, G. L.; Peterson, J. A.; McCormick, D. J.; Fauq, A. H.; Khan, M. A.; Wengenack, T. M. *Biochemistry* **2004**, *43*, 6064.
13. Bacskai, B. J.; Frosch, M. P.; Freeman, S. H.; Raymond, S. B.; Augustinack, J. C.; Johnson, K. A.; Irizarry, M. C.; Klunk, W. E.; Mathis, C. A.; Dekosky, S. T.; Greenberg, S. M.; Hyman, B. T.; Growdon, J. H. *Arch. Neurol.* **2007**, *64*, 431.
14. Johnson, K. A.; Gregas, M.; Becker, J. A.; Kinnecom, C.; Salat, D. H.; Moran, E. K.; Smith, E. E.; Rosand, J.; Rentz, D. M.; Klunk, W. E.; Mathis, C. A.; Price, J. C.; Dekosky, S. T.; Fischman, A. J.; Greenberg, S. M. *Ann. Neurol.* **2007**, *62*, 229.
15. Pike, K. E.; Savage, G.; Villemagne, V. L.; Ng, S.; Moss, S. A.; Maruff, P.; Mathis, C. A.; Klunk, W. E.; Masters, C. L.; Rowe, C. C. *Brain* **2007**, *130*, 2837.
16. Hintersteiner, M.; Enz, A.; Frey, P.; Jaton, A. L.; Kinzy, W.; Kneuer, R.; Neumann, U.; Rudin, M.; Staufenbiel, M.; Stoeckli, M.; Wiederhold, K. H.; Gremlich, H. U. *Nat. Biotechnol.* **2005**, *23*, 577.
17. Nesterov, E. E.; Skoch, J.; Hyman, B. T.; Klunk, W. E.; Bacskai, B. J.; Swager, T. M. *Angew. Chem., Int. Ed. Engl.* **2005**, *44*, 5452.
18. Raymond, S. B.; Skoch, J.; Hills, I. D.; Nesterov, E. E.; Swager, T. M.; Bacskai, B. J. *Eur. J. Nucl. Med. Mol. Imaging* **2008**, *35*, S93.
19. Hrobarik, P.; Sigmundova, I.; Zahradnik, P. *Synthesis* **2005**, *4*, 600.
20. Cho, B. R.; Chajara, K.; Jung, H.; Son, K. H.; Jeon, S. J. *Org. Lett.* **2002**, *4*, 1703.
21. Toyama, H.; Ye, D.; Ichise, M.; Liow, J. S.; Cai, L.; Jacobowitz, D.; Musachio, J. L.; Hong, J.; Crescenzo, M.; Tipre, D.; Lu, J. Q.; Zoghbi, S.; Vines, D. C.; Seidel, J.; Katada, K.; Green, M. V.; Pike, V. W.; Cohen, R. M.; Innis, R. B. *Eur. J. Nucl. Med. Mol. Imaging* **2005**, *32*, 593.

Novel Radioiodinated Aurones as Probes for SPECT Imaging of β-Amyloid Plaques in the Brain

Yoshifumi Maya,[†] Masahiro Ono,*[,†,‡] Hiroyuki Watanabe,[†] Mamoru Haratake,[†] Hideo Saji,[‡] and Morio Nakayama*[,†]

Department of Hygienic Chemistry, Graduate School of Biomedical Sciences, Nagasaki University, 1-14 Bunkyo-machi, Nagasaki 852-8521, and Department of Patho-Functional Bioanalysis, Graduate School of Pharmaceutical Sciences, Kyoto University, 46−29 Yoshida Shimoadachi-cho, Sakyo-ku, Kyoto 606-8501, Japan. Received July 29, 2008; Revised Manuscript Received November 10, 2008

We report a novel series of radioiodinated aurone derivatives as probes for imaging Aβ plaques in the brains of patients with Alzheimer's disease (AD) using single photon emission computed tomography (SPECT). In binding experiments in vitro, aurone derivatives showed very good affinity for Aβ aggregates (K_i = 1.1 to 3.4 nM). No-carrier-added radioiodinated aurones were successfully prepared through an iododestannylation reaction from the corresponding tributyltin derivatives. In biodistribution experiments using normal mice, aurone derivatives displayed high brain uptake (1.7−4.5% ID/g at 2 min) and rapid clearance from the brain (0.1−0.4% ID/g at 30 min), especially [^{125}I]**15**. Furthermore, a specific plaque labeling signal was observed in in vitro autoradiography of postmortem AD brain sections using [^{125}I]**15**. [^{125}I]**15** may be a useful SPECT imaging agent for detecting Aβ plaques in the brain of AD.

INTRODUCTION

Alzheimer's disease (AD) is a progressive neurodegenerative disorder characterized by cognitive decline, irreversible memory loss, disorientation, and language impairment. Senile plaques containing β-amyloid (Aβ) peptides and neurofibrillary tangles in the postmortem brain are two pathological hallmarks of AD (*1, 2*). Excessive production of Aβ via various normal or abnormal mechanisms is considered to be the initial neurodegenerative event in AD. Currently, it is difficult for clinicians to differentiate between the cognitive decline associated with normal aging and the cognitive decline associated with AD. There is no simple and definitive diagnostic method to detect Aβ plaques in the brain without postmortem pathological staining of brain tissue. Thus, the development of imaging agents for positron emission tomography (PET) or single photon emission computed tomography (SPECT), which can detect Aβ plaques in vivo, may assist with the early diagnosis of AD (*3−5*).

In the past few years, several groups have reported potential amyloid-imaging probes for the detection of Aβ plaques in vivo. Tracers such as [^{11}C]PIB (*6, 7*), [^{11}C]SB-13 (*8, 9*), [^{18}F]BAY94-9172 (*10*), [^{11}C]BF-227 (*11*), [^{18}F]FDDNP (*12−14*), and [^{123}I]IMPY (*15−18*) have been tested clinically and demonstrated utility (Figure 1). [^{123}I]IMPY is the only tracer for SPECT; the other five tracers are amyloid imaging probes for PET. Since SPECT is more valuable than PET in terms of routine diagnostic use, the development of more useful β-amyloid-imaging agents for SPECT has been a critical issue.

Recently, we have reported that radioiodinated aurones possessing a nucleophilic group (NH_2, NHMe, and NMe_2) function as a new backbone structure in the development of amyloid-imaging probes for SPECT (*19*). These compounds showed strong binding to Aβ aggregates (K_i = 1.2−6.8 nM), good penetration of the brain (1.9−4.6% ID/g at 2 min), and a fast washout from the brain (0.3−0.5% ID/g at 30 min). However, the aurone derivatives appeared inferior to IMPY in pharmacokinetics, although their high affinity for β-amyloid plaques is sufficient for imaging in vivo. Therefore, additional structural changes are essential to further improve the properties of aurone derivatives to make them suitable for the imaging of β-amyloid plaques in the brain.

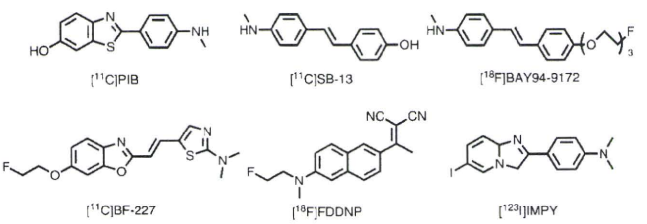

Figure 1. Chemical structure of Aβ imaging probes clinically tested.

To develop more promising aurones for SPECT-based imaging of β-amyloid plaques, we designed a novel series of radioiodinated derivatives with poly(ethylene glycol) (PEG). PEG is nontoxic, nonimmunogenic, highly soluble in water, and FDA-approved, and PEGylation has been used to change the pharmacokinetics of various biologically interesting proteins or peptides, leading to better therapeutics (*20, 21*). Therefore, PEGylated aurone derivatives are worthy of further evaluation as novel β-amyloid-imaging probes for SPECT.

In the present study, we designed and synthesized a novel series of radioiodinated aurone derivatives with not only 1 to 3 units of ethylene glycol at the 4′ position, but also other nucleophilic groups (-OCH_3 and -OH), and evaluated their biological potential as probes for imaging β-amyloid by testing their affinity for Aβ aggregates in vitro and their uptake by and

* To whom correspondence should be addressed. Phone +81-75-753-4608, Fax +81-75-753-4568, e-mail ono@pharm.kyoto-u.ac.jp for M. Ono. Phone +81-95-819-2441, Fax +81-95-819-2441, e-mail morio@nagasaki-u.ac.jp for M. Nakayama.

† Nagasaki University.

‡ Kyoto University.

10.1021/bc8003292 CCC: $40.75
Published on Web 12/11/2008

clearance from the brain in biodistribution experiments using normal mice.

MATERIALS AND METHODS

All reagents were commercial products and used without further purification unless otherwise indicated. ^{1}H NMR spectra were obtained on a Varian Gemini 300 spectrometer with TMS as an internal standard. Coupling constants are reported in hertz. Multiplicity was defined by s (singlet), d (doublet), t (triplet), and m (multiplet). Mass spectra were obtained on a JEOL IMS-DX instrument.

Chemistry. *Methyl 2-((Ethoxycarbonyl)methoxy)-5-bromobenzoate (**1**).* To a solution of 2-hydroxy-5-bromobenzoic acid methyl ester (1.5 g, 6.49 mmol) in acetone (10 mL) was added K_2CO_3 (2.7 g, 19.5 mmol) and ethylbromoacetate (1.3 mL, 7.78 mmol). The mixture was stirred for 3 h under reflux. After the solvent was evaporated, the residue was dissolved in water (100 mL) and extracted with ethyl acetate (100 mL). The organic layer was dried over Na_2SO_4, and evaporation of the solvent gave 1.60 g of **1** (77.7%). ^{1}H NMR NMR (300 MHz, $CDCl_3$) δ 1.29 (t, J = 7.2 Hz, 3H), 3.91 (s, 3H), 4.24 (q, J = 7.2 Hz, 2H), 4.69 (s, 2H), 6.78 (d, J = 9.0 Hz, 1H), 7.54 (d, J = 6.3 Hz, 1H), 7.96 (s, 1H).

*2-(Carboxymethoxy)-5-bromobenzoic Acid (**2**).* To a solution of **1** (1.6 g, 5.04 mmol) in methanol (10 mL) was added 10% aqueous KOH (3.0 mL). The mixture was stirred for 2 h at room temperature. The product formed by adding 1 N HCl was filtered to give 1.10 g of **2** (79.4%). ^{1}H NMR (300 MHz, CD_3OD) δ 4.81 (s, 2H), 7.02 (d, J = 8.7 Hz, 1H), 7.63 (dd, J = 2.4, 2.7 Hz, 1H), 7.93 (d, J = 2.4 Hz, 1H).

*5-Bromo-3-acetoxybenzofuran (**3**).* A mixture of acetic anhydride (20 mL), acetic acid (4 mL), anhydrous sodium acetate (1.0 g, 12.0 mmol), and **2** (100 mg, 0.36 mmol) was heated to reflux for 5 h. Water (100 mL) was then added, and the mixture was extracted with chloroform (100 mL). After drying of the organic layer on Na_2SO_4, evaporation gave 78 mg of **3** (86.5%). ^{1}H NMR (300 MHz, $CDCl_3$) δ 2.37 (s, 3H), 7.33 (d, J = 9.0 Hz, 1H), 7.43 (dd, J = 3.6, 2.1 Hz, 1H), 7.71 (s, 1H), 8.02 (s, 1H).

*5-Bromobenzofuran-3(2H)-one (**4**).* A mixture of **3** (78 mg, 0.31 mmol), methanol (3 mL), water (1 mL), and 1 N HCl (2 mL) was heated to reflux for 3 h. The precipitate formed was collected by filtration, washed with water, and dried under vacuum to obtain 15 mg of **4** (22.5%). ^{1}H NMR (300 MHz, $CDCl_3$) δ 4.67 (s, 2H), 7.06 (d, J = 9.0 Hz, 1H), 7.69 (dd, J = 2.1, 2.1 Hz, 1H), 7.79 (d, J = 2.1 Hz, 1H).

*(Z)-2-(4-Methoxybenzylidene)-5-bromobenzofuran-3(2H)-one (**5**).* To a solution of **4** (300 mg, 1.41 mmol) and 4-methoxybenzaldehyde (192 mg, 1.41 mmol) in chloroform (5 mL) was added Al_2O_3 (2.7 g, 26.0 mmol). The mixture was stirred for 20 min at room temperature. After filtration of the reaction mixture, the solvent of the filtrate was removed, and drying under vacuum yielded 410 mg of **5** (85.7%). ^{1}H NMR (300 MHz, $CDCl_3$) δ 3.88 (s, 3H), 6.91 (s, 1H), 6.99 (d, J = 9.0 Hz, 2H), 7.24 (d, J = 8.4 Hz, 1H), 7.73 (dd, J = 2.1, 2.1 Hz, 1H), 7.88 (d, J = 8.7 Hz, 2H), 7.92 (d, J = 1.8 Hz, 1H).

*(Z)-2-(4-Hydroxybenzylidene)-5-bromobenzofuran-3(2H)-one (**6**).* BBr_3 (3 mL, 1 M solution in CH_2Cl_2) was added to a solution of **5** (300 mg, 0.91 mmol) in CH_2Cl_2 (25 mL) dropwise in an ice bath. The mixture was allowed to warm to room temperature and stirred for 15 h. Water (50 mL) was added while the reaction mixture was cooled in an ice bath. The mixture was extracted with chloroform (2 × 30 mL), and the organic phase was dried over Na_2SO_4 and filtered. The filtrate was concentrated and the residue was purified by silica gel chromatography (hexane/ethyl acetate = 2:3) to give 15 mg of **6** (5.2%). ^{1}H NMR (300 MHz, DMSO-d_6) δ 1.23 (s, 1H), 6.92 (d, J = 8.4 Hz, 2H), 6.96 (s, 1H), 7.56 (d, J = 9.3 Hz, 1H), 7.88−7.92 (m, 3H), 7.95 (s, 1H). MS (EI) m/z 316 [M^+].

*(Z)-2-(4-Methoxybenzylidene)-5-(tributylstannyl)benzofuran-3(2H)-one (**7**).* A mixture of **5** (200 mg, 0.60 mmol), $(Bu_3Sn)_2$ (0.4 mL), and $(Ph_3P)_4Pd$ (50 mg, 0.043 mmol) in a mixed solvent (15 mL, 1:1 dioxane/Et_3N) was stirred under reflux for 24 h. The solvent was removed, and the resulting residue was purified by silica gel chromatography using chloroform to give 50 mg of **7** (15.3%). ^{1}H NMR (300 MHz, $CDCl_3$) δ 0.89−1.64 (m, 27H), 3.87 (s, 3H), 6.89 (s, 1H), 6.99 (d, J = 8.7 Hz, 2H), 7.31 (d, J = 8.1 Hz, 1H), 7.71 (dd, J = 0.9, 0.9 Hz, 1H), 7.86 (d, J = 9.0 Hz, 2H), 7.90 (d, J = 8.7 Hz 1H). MS (EI) m/z 528 [M^+].

*(Z)-2-(4-Hydroxybenzylidene)-5-(tributylstannyl)benzofuran-3(2H)-one (**8**).* The same reaction as described above to prepare **7** was used, and 10 mg of **8** was obtained in a 12.0% yield from **6**. ^{1}H NMR (300 MHz, $CDCl_3$) δ 0.86−1.60 (m, 27H), 6.74 (d, J = 9.0 Hz, 2H), 6.90 (s, 1H), 7.30 (d, J = 8.1 Hz, 1H), 7.69 (d, J = 8.1 Hz, 1H), 7.80 (d, J = 8.4 Hz, 2H), 7.89 (s, 1H). MS (EI) m/z 542 [M^+].

*(Z)-2-(4-Methoxybenzylidene)-5-iodobenzofuran-3(2H)-one (**9**).* To a solution of **7** (10 mg, 0.03 mmol) in $CHCl_3$ (3 mL) was added a solution of iodine in $CHCl_3$ (1 mL, 0.25 M) at room temperature. The mixture was stirred at room temperature for 5 min, and saturated $NaHSO_3$ solution (15 mL) was added. The organic phase was separated, dried over Na_2SO_4, and filtered. The solvent was removed, and the residue was purified by preparative TLC (2:3 hexane/ethyl acetate) to give 6 mg of **9** (84.0%). ^{1}H NMR (300 MHz, $CDCl_3$) δ 3.88 (s, 3H), 6.91 (s, 1H), 6.98 (d, J = 6.9 Hz, 2H), 7.14 (d, J = 8.4 Hz, 1H), 7.87−7.91 (m, 3H), 8.12 (d, J = 2.1 Hz, 1H). HRMS (EI) m/z calcd for $C_{16}H_{11}O_3I$ (M^+) 377.9753, found 377.9753.

*Methyl 2-((Ethoxycarbonyl)methoxy)-5-iodobenzoate (**10**).* The same reaction as described above to prepare **1** was used, and 2.62 g of **10** was obtained in a 99.0% yield from 2-hydroxy-5-iodobenzoic acid methyl ester. ^{1}H NMR (300 MHz, $CDCl_3$) δ 1.29 (t, J = 7.2 Hz, 3H), 3.90 (s, 3H), 4.25 (q, J = 6.0 Hz, 2H), 4.69 (s, 2H), 6.66 (d, J = 8.7 Hz, 1H), 7.71 (dd, J = 2.4, 2.4 Hz, 1H), 8.12 (d, J = 2.1 Hz, 1H).

*2-(Carboxymethoxy)-5-iodobenzoic Acid (**11**).* The same reaction as described above to prepare **2** was used, and 2.02 g of **11** was obtained in a 87.2% yield from **10**. ^{1}H NMR (300 MHz, CD_3OD) δ 4.81 (s, 2H), 6.89 (d, J = 9.0 Hz, 1H), 7.80 (dd, J = 2.7, 2.4 Hz, 1H), 8.10 (d, J = 2.4 Hz, 1H).

*5-Iodo-3-acetoxybenzofuran (**12**).* The same reaction as described above to prepare **3** was used, and 1.45 g of **12** was obtained in a 76.6% yield from **11**. ^{1}H NMR (300 MHz, $CDCl_3$) δ 2.37 (s, 3H), 7.23 (d, J = 8.1 Hz, 1H), 7.59 (dd, J = 1.5, 1.8 Hz, 1H), 7.90 (d, J = 1.5 Hz, 1H), 7.98 (s, 1H).

*5-Iodobenzofuran-3(2H)-one (**13**).* The same reaction as described above to prepare **4** was used, and 1.17 g of **13** was obtained in a 93.8% yield from **12**. ^{1}H NMR (300 MHz, $CDCl_3$) δ 4.65 (s, 2H), 6.96 (d, J = 9.0 Hz, 1H), 7.85 (dd, J = 1.8, 1.8 Hz, 1H), 7.99 (d, J = 1.8 Hz, 1H).

*(Z)-2-(4-Hydroxybenzylidene)-5-iodobenzofuran-3(2H)-one (**14**).* The same reaction as described above to prepare **5** was used, and 78 mg of **14** was obtained in a 87.0% yield from **13** and 4-hydroxybenzaldehyde. ^{1}H NMR (300 MHz, $CDCl_3$) δ 1.28 (s, 1H), 6.87 (s, 1H), 6.91 (d, J = 5.4 Hz, 2H), 7.29 (d, J = 8.7 Hz, 1H), 7.85 (d, J = 6.9 Hz, 2H), 8.12 (d, J = 6.9 Hz, 1H), 8.08 (d, J = 1.8 Hz, 1H). HRMS (EI) m/z calcd for $C_{15}H_9O_3I$ (M^+) 363.9596, found 363.9571.

*(Z)-2-(4-(2-Hydroxyethoxy)benzylidene)-5-iodobenzofuran-3(2H)-one (**15**).* A mixture of potassium carbonate (3.7 g, 26.8 mmol), **14** (194 mg, 0.53 mmol), and ethylene chlorohydrin (0.1 mL, 1.43 mmol) in anhydrous DMF (7 mL) was heated at 120 °C for 15 h. After cooling to room temperature, water was added,

and the reaction mixture was extracted with ethyl acetate. The organic layer was separated, dried over Na_2SO_4, and evaporated. The resulting residue was purified by silica gel chromatography using ethyl acetate to give 123 mg of **15** (56.5%). ^{1}H NMR (300 MHz, $CDCl_3$) δ 2.01 (s, 1H), 4.02 (s, 2H), 4.18 (t, J = 3.9 Hz, 2H), 6.89 (s, 1H), 7.00 (d, J = 7.5 Hz, 2H), 7.14 (d, J = 8.4 Hz, 1H), 7.80−7.92 (m, 3H), 8.12 (d, J = 1.8 Hz, 1H). HRMS (EI) *m/z* calcd for $C_{17}H_{13}O_4I$ (M^+) 407.9859, found 407.9879.

*(Z)-2-(4-(2-(2-Hydroxyethoxy)ethoxy)benzylidene)-5-iodobenzofuran-3(2H)-one (**16**).* The same reaction as described above to prepare **15** was used, and 56 mg of **16** was obtained in a 30.2% yield from **14** and ethylene glycol mono-2-chloroethyl ether. ^{1}H NMR (300 MHz, $CDCl_3$) δ 2.17 (s, 1H), 3.70 (d, J = 4.8 Hz, 2H), 3.78 (d, J = 4.8 Hz, 2H), 3.92 (t, J = 4.8 Hz, 2H), 4.21 (t, J = 4.5 Hz, 2H), 6.89 (s, 1H), 7.00 (d, J = 11.4 Hz, 2H), 7.13 (d, J = 8.7 Hz, 1H), 7.84−7.91 (m, 3H), 8.11 (d, J = 2.1 Hz, 1H). HRMS (EI) *m/z* calcd for $C_{19}H_{17}O_5I$ (M^+) 452.0121, found 452.0131.

*(Z)-2-(4-(2-(2-(2-Hydroxyethoxy)ethoxy)ethoxy)benzylidene)-5-iodobenzofuran-3(2H)-one (**17**).* The same reaction as described above to prepare **15** was used, and 140 mg of **17** was obtained in a 67.9% yield from **14** and 2-[2-(2-chloroethoxy)ethoxy] ethanol. ^{1}H NMR (300 MHz, $CDCl_3$) δ 1.96 (s, 1H), 3.74−3.80 (m, 6H), 3.92 (t, J = 4.8 Hz, 2H), 4.24 (t, J = 4.8 Hz, 2H), 4.45 (t, J = 4.5 Hz, 1H), 4.65 (t, J = 4.5 Hz, 1H), 6.91 (s, 1H), 6.98 (d, J = 9.0 Hz, 2H), 7.15 (d, J = 8.7 Hz, 1H), 7.85−7.92 (m, 3H), 8.15 (d, J = 2.1 Hz, 1H). HRMS (EI) *m/z* calcd for $C_{21}H_{21}O_6I$ (M^+) 496.0383, found 496.0381.

*(Z)-2-(4-(2-Hydroxyethoxy)benzylidene)-5-(tributylstannyl)benzofuran-3(2H)-one (**18**).* The same reaction as described above to prepare **7** was used, and 7 mg of **18** was obtained in a 25.0% yield from **15**. ^{1}H NMR (300 MHz, $CDCl_3$) δ 0.86−1.61 (m, 27H), 2.06 (s, 1H), 4.02 (s, 2H), 4.16 (t, J = 3.6 Hz, 2H), 6.88 (s, 1H), 6.99 (d, J = 9.0 Hz, 2H), 7.30 (d, J = 12.3 Hz, 1H), 7.73 (d, J = 9.0 Hz, 1H), 7.90−7.92 (m, 3H). MS (EI) *m/z* 572 [M^+].

*(Z)-2-(4-(2-(2-Hydroxyethoxy)ethoxy)benzylidene)-5-(tributylstannyl)benzofuran-3(2H)-one (**19**).* The same reaction as described above to prepare **7** was used, and 17 mg of **19** was obtained in a 31.4% yield from **16**. ^{1}H NMR (300 MHz, $CDCl_3$) δ 0.86−1.32 (m, 27H), 2.11 (s, 1H), 3.70 (t, J = 4.8 Hz, 2H), 3.78 (t, J = 4.8 Hz, 2H), 3.91 (t, J = 4.5 Hz, 2H), 4.22 (t, J = 5.1 Hz, 2H), 6.89 (s, 1H), 7.00 (d, J = 7.2 Hz, 2H), 7.31 (d, J = 8.1 Hz, 1H), 7.71 (d, J = 9.0 Hz, 1H), 7.88−7.91 (m, 3H). MS (EI) *m/z* 616 [M^+].

*(Z)-2-(4-(2-(2-(2-Hydroxyethoxy)ethoxy)ethoxy)benzylidene)-5-(tributylstannyl)benzofuran-3(2H)-one (**20**).* The same reaction as described above to prepare **7** was used, and 4 mg of **20** was obtained in a 30.3% yield from **17**. ^{1}H NMR (300 MHz, $CDCl_3$) δ 0.86−1.59 (m, 27H), 2.11 (s, 1H), 3.63 (t, J = 3.3 Hz, 2H), 3.73−3.75 (m, 4H), 3.90 (t, J = 4.2 Hz, 2H), 4.21 (t, J = 4.2 Hz, 2H), 6.88 (s, 1H), 7.10 (d, J = 8.7 Hz, 2H), 7.31 (d, J = 8.1 Hz, 1H), 7.64−7.70 (m, 3H), 7.90 (d, J = 4.8 Hz, 1H). MS (EI) *m/z* 659 [M^+].

Iododestannylation Reaction. The radioiodinated forms of compounds **9**, **14**, **15**, **16**, and **17** were prepared from the corresponding tributyltin derivatives by iododestannylation. Briefly, to initiate the reaction, the tributyltin derivative (50 μg/50 μL EtOH) was added to a mixture of a [^{125}I]NaI (3.7−7.4 MBq, specific activity 2200 Ci/mmol), 50 μL of H_2O_2 (3%), and 50 μL of 1 N HCl in a sealed vial. The reaction was allowed to proceed at room temperature for 2 min and was terminated by addition of $NaHSO_3$. The reaction, after neutralization with sodium bicarbonate, was extracted with ethyl acetate. The extract was dried by passing through an anhydrous Na_2SO_4 column and was then blown dry with a stream of nitrogen gas. The radioiodinated ligand was purified by HPLC on a Cosmosil C_{18} column with an isocratic solvent of H_2O/acetonitrile (3:7) at a flow rate of 1.0 mL/min.

Binding Assays Using the Aggregated Aβ Peptide in Solution. A solid form of Aβ(1−42) was purchased from Peptide Institute (Osaka, Japan). Aggregation was carried out by gently dissolving the peptide (0.25 mg/mL) in a buffer solution (pH 7.4) containing 10 mM sodium phosphate and 1 mM EDTA. The solution was incubated at 37 °C for 42 h with gentle and constant shaking. (Z)-2-(4-Aminobenzylidene)-5-iodobenzofuran-3(2*H*)-one ([^{125}I]AAU) was synthesized and used as the radioligand for the competition binding experiments (K_d value of [^{125}I]AAU is 4.2 nM) (*19*). The binding experiments were carried out in 12 × 75 mm borosilicate glass tubes according to a procedure described previously (*19*). A mixture containing 50 μL of test compound (0.8 nM−12.5 μM in 10% ethanol), 50 μL of 0.02 nM [^{125}I]AAU, 50 μL of Aβ(1−42) aggregate, and 850 μL of 10% ethanol was incubated at room temperature for 3 h. The mixture was then filtered through Whatman GF/B filters using a Brandel M-24 cell harvester, and the filters containing the bound ^{125}I ligand were placed in a gamma counter. Values for the half-maximal inhibitory concentration (IC_{50}) were determined from displacement curves of three independent experiments using GraphPad *Prism* 4.0, and those for the inhibition constant (K_i) were calculated using the Cheng-Prusoff equation (*22*): $K_i = IC_{50}/(1 + [L]/K_d)$, where [L] is the concentration of [^{125}I]AAU used in the assay, and K_d is the dissociation constant of AAU (4.2 nM) (*19*).

Staining of Amyloid Plaques in Transgenic Mouse Brain Sections. Tg2576 transgenic mice (20 month of age) were used as an Alzheimer's model. The brain was removed and sliced into serial sections 10 μm thick. Each slide was incubated with a 50% ethanol solution of compound **9**, **14**, **15**, **16**, and **17** (100 μM). Finally, the sections were washed in 50% EtOH for 3 min two times. Fluorescent observation was performed with the Nikon system (Excitation filter, 450−490 nm; Dichroic mirror, DM505; Barrier filter, BA520). Thereafter, the serial sections were also stained with thioflavin S, a pathological dye commonly used for staining Aβ plaques in the brain.

In Vivo Biodistribution in Normal Mice. Animal studies were conducted in accordance with our institutional guidelines and were approved by Nagasaki University Animal Care Committee. A saline solution (100 μL) containing radiolabeled agents (4.2−6.3 kBq) and 10% ethanol was intravenously injected directly into the tail vein of ddY mice (5 weeks old, average weight 20−25 g). The mice were sacrificed at various time points postinjection. The organs of interest were removed and weighed, and the radioactivity was measured with an automatic gamma counter (Aloka, ARC-380). Percent dose per gram of samples was calculated by comparing the sample counts with the counts of the initial dose.

In Vitro Autoradiography. Postmortem brain tissues from an autopsy-confirmed case of AD (73-year-old male) and a control subject (36-year-old male) were obtained from BioChain Institute Inc. The presence and localization of plaques on the sections were confirmed with immunohistochemical staining using a monoclonal Aβ antibody BC05 (Wako) as reported (*23*). The sections were incubated with [^{125}I]**15** (120000 cpm/100 μL) for 1 h at room temperature. They were then dipped in saturated lithium carbonate in 40% EtOH (two 2-min washes) and washed with 40% EtOH (one 2-min wash), before being rinsed with water for 30 s. After drying, the ^{125}I-labeled sections were exposed to a Fuji Film imaging plate overnight.

RESULTS AND DISCUSSION

Chemistry. The target aurone derivatives (**9**, **14**, **15**, **16**, and **17**) were prepared as shown in Schemes 1−3. The synthesis of

Scheme 1

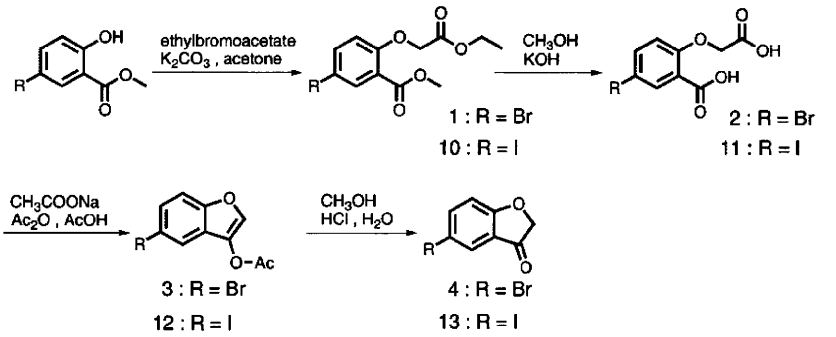

Scheme 2

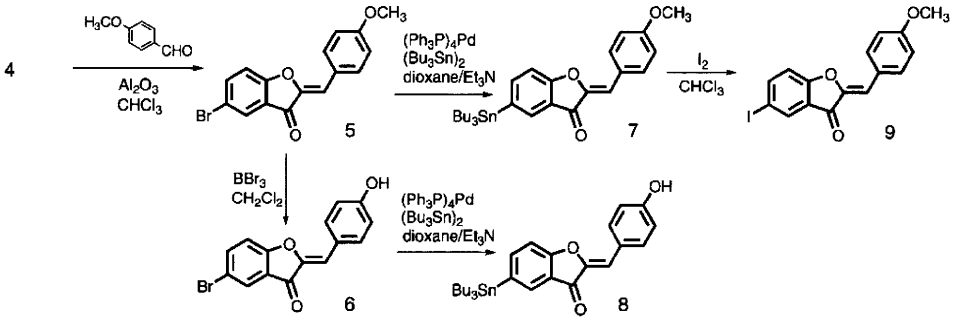

Scheme 3

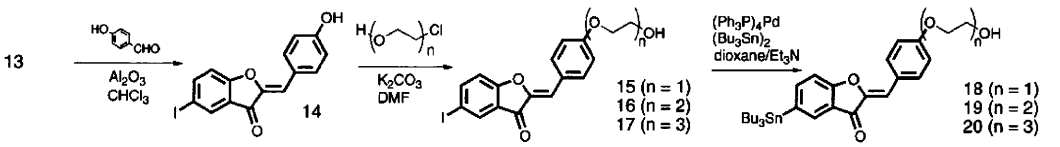

the aurone backbone was achieved by an Aldol reaction of benzofuranones with benzaldehydes using Al_2O_3 (*23*). In this process, benzofuranones were reacted with methoxy benzaldehyde or hydroxy benzaldehyde in the presence of Al_2O_3 in chloroform at room temperature to form compounds **5** and **14** in yields of 85.7% and 87.0%, respectively. Compound **5** was converted to **6** by demethylation with BBr_3 in CH_2Cl_2 (5.2% yields). Direct alkylation of **14** with ethylene chlorohydrin, ethylene glycol mono-2-chloroethyl ether, or 2-[2-(2-chloroethoxy)ethoxy]ethanol with potassium carbonate in DMF resulted in **15**, **16**, and **17**, respectively. The tributyltin derivatives (**7**, **8**, **18**, **19**, and **20**) were prepared from the corresponding compounds (**5**, **6**, **15**, **16**, and **17**) using a halogen to tributyltin exchange reaction catalyzed by Pd(0) for yields of 15.3%, 12.0%, 25.0%, 31.4%, and 30.3%, respectively. The tributyltin derivatives were used as the starting materials for radioiodination in the preparation of [^{125}I]**9**, [^{125}I]**14**, [^{125}I]**15**, [^{125}I]**16**, and [^{125}I]**17**. Novel radioiodinated aurones were achieved by an iododestannylation reaction using hydrogen peroxide as the oxidant, which produced the desired radioiodinated ligands (Scheme 4). It was anticipated that the no-carrier-added preparation would result in a final product bearing a theoretical specific activity similar to that of ^{125}I (2200 Ci/mmol). The radiochemical identities of the radioiodinated ligands were verified by coinjection with nonradioactive compounds by their HPLC profiles (Supporting Information). Five radioiodinated products were obtained in 25−57% radiochemical yields with radiochemical purities of >95% after purification by HPLC.

Binding Experiments Using Aβ Aggregates in Vitro. Our initial screening of the affinity of aurone derivatives (**9**, **14**, **15**, **16**, and **17**) was carried out with Aβ(1−42) aggregates, using

Scheme 4

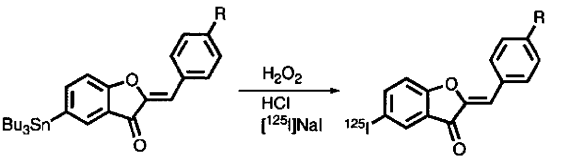

7
8
18
19
20

[^{125}I]9 (R = OCH_3)
[^{125}I]14 (R = OH)
[^{125}I]15 (R = OCH_2CH_2OH)
[^{125}I]16 (R = $(OCH_2CH_2)_2OH$)
[^{125}I]17 (R = $(OCH_2CH_2)_3OH$)

[^{125}I]AAU as the competing radioligand (Table 1). The K_i values estimated for **9**, **14**, **15**, **16**, and **17** were 2.9, 1.3, 1.1, 3.4, and 2.6 nM, respectively. These values suggested that the new series of aurone derivatives had binding affinity for Aβ(1−42) aggregates despite their substituted groups. The binding affinity is in the same range as that of aurone derivatives possessing a nucleophilic group (NH_2, NHMe, NMe_2), reported previously

Table 1. Inhibition Constants (K_i) of Newly Synthesized Aurone Derivatives for the Binding of Ligands to Aβ (1−42) Aggregates

compound	K_i (nM)[a]
9	2.89 ± 0.42
14	1.28 ± 0.29
15	1.05 ± 0.06
16	3.36 ± 0.29
17	2.56 ± 0.31

[a] Data are the mean ± SEM for two independent measurements done in triplicate.

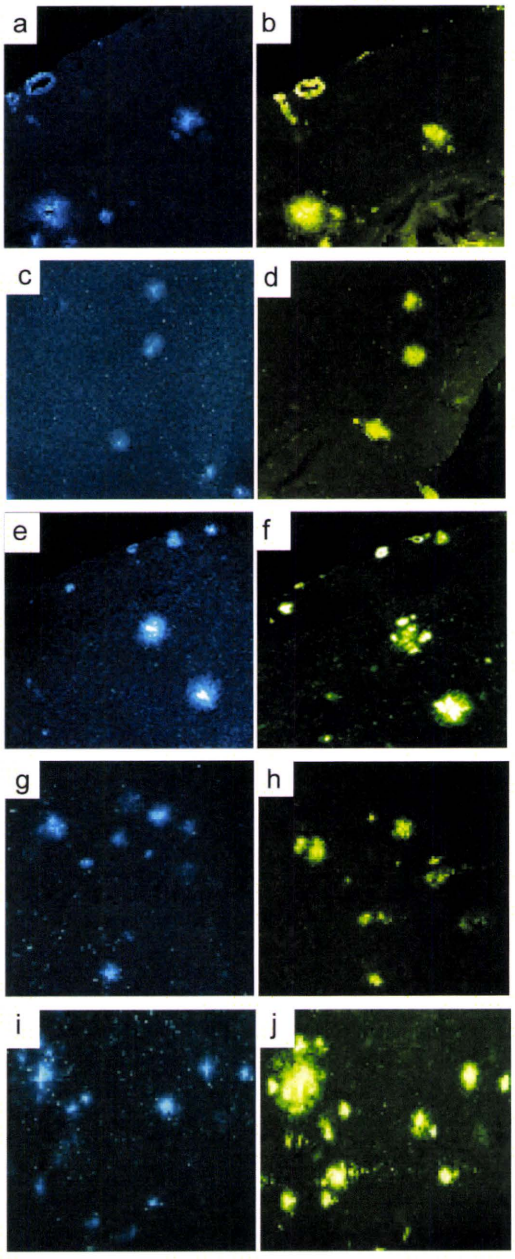

Figure 2. Neuropathological staining of **9**, **14**, **15**, **16**, and **17** (a, c, e, g, and i) in 10 μm sections from a mouse model of AD. Labeled plaques were confirmed by staining of the adjacent sections with thioflavin S (b, d, f, h, and j).

(*19*). These results clearly indicated that there exists considerable tolerance for structural modifications of aurone derivatives. The binding affinity of aurone derivatives is very close to that of known β-amyloid-imaging agents such as SB-13 (K_i = 1.2 nM) (*24*), PIB (K_i = 2.8 nM) (*25*), and IMPY (K_i = 1.4 nM) (*24*), indicating that they have strong enough affinity to test clinically.

Neuropathological Staining of Mouse Brain Sections. To confirm the affinity of aurone derivatives for β-amyloid plaques in the mouse brain, neuropathological fluorescent staining with **9**, **14**, **15**, **16**, and **17** was carried out using double transgenic Alzheimer's mouse brain sections (Figure 2). Many amyloid plaques were clearly stained with the derivatives, as reflected by the high binding affinity for Aβ aggregates in in vitro competition assays. The labeling pattern was consistent with that observed with thioflavin S. These results suggest that novel aurone derivatives show affinity for β-amyloid plaques in the mouse brain in addition to having binding affinity for synthetic Aβ42 aggregates.

Table 2. Biodistribution of Radioactivity after Injection of Aurone Derivatives in Normal Mice[a]

	time after injection (min)			
tissue	2	10	30	60
		[^{125}I]**9**		
blood	3.16 (0.82)	1.51 (0.23)	0.95 (0.19)	0.70 (0.60)
liver	6.87 (2.18)	5.16 (0.73)	2.76 (0.40)	1.86 (0.83)
kidney	7.26 (2.18)	7.00 (1.49)	4.93 (1.52)	2.43 (1.17)
intestine	1.59 (0.51)	4.70 (1.46)	11.67 (3.56)	9.02 (3.14)
spleen	1.45 (0.56)	0.74 (0.10)	0.48 (0.10)	0.43 (0.14)
pancreas	2.83 (0.75)	0.77 (0.17)	0.62 (0.75)	0.16 (0.05)
heart	3.84 (1.04)	1.06 (0.10)	0.37 (0.09)	0.25 (0.12)
stomach[b]	0.39 (0.20)	0.89 (0.48)	0.42 (0.13)	0.82 (0.46)
brain	1.69 (0.43)	0.54 (0.12)	0.11 (0.05)	0.03 (0.02)
		[^{125}I]**14**		
blood	3.14 (0.39)	2.77 (0.28)	1.75 (0.38)	0.87 (0.28)
liver	6.05 (1.49)	6.63 (1.08)	4.23 (0.63)	4.45 (3.14)
kidney	11.08 (2.96)	11.22 (2.26)	5.82 (1.11)	2.43 (1.04)
intestine	2.11 (0.75)	6.12 (0.83)	12.67 (2.13)	14.87 (5.42)
spleen	2.18 (0.48)	1.36 (0.83)	0.69 (0.14)	0.42 (0.02)
pancreas	5.28 (0.99)	2.65 (0.64)	0.92 (0.19)	0.36 (0.09)
heart	6.23 (0.63)	2.57 (0.41)	0.98 (0.14)	0.42 (0.14)
stomach[b]	0.93 (0.28)	1.46 (0.23)	1.22 (0.72)	1.89 (1.01)
brain	3.07 (0.39)	1.48 (0.19)	0.37 (0.07)	0.14 (0.12)
		[^{125}I]**15**		
blood	4.97 (0.96)	3.88 (1.09)	2.38 (0.85)	1.24 (0.35)
liver	13.4 (3.20)	13.3 (2.59)	7.60 (1.95)	5.27 (0.64)
kidney	11.3 (1.23)	10.8 (2.58)	6.09 (2.43)	2.50 (1.30)
intestine	2.78 (0.42)	7.83 (2.22)	17.82 (3.58)	20.93 (4.46)
spleen	2.72 (0.28)	1.02 (0.22)	0.50 (0.13)	0.21 (0.09)
pancreas	6.38 (0.63)	1.61 (0.61)	0.59 (0.21)	0.29(0.15)
heart	6.30 (0.65)	2.30 (0.46)	0.83 (0.15)	0.72 (0.58)
stomach[b]	1.88 (0.41)	3.23 (2.58)	5.15 (4.43)	1.45 (0.78)
brain	4.51 (0.25)	1.48 (0.28)	0.24 (0.03)	0.09 (0.04)
		[^{125}I]**16**		
blood	3.61 (0.74)	5.18 (2.54)	1.11 (0.73)	0.68 (0.45)
liver	12.5 (3.21)	11.6 (1.75)	9.31 (2.66)	7.12 (4.05)
kidney	12.0 (0.99)	10.3 (1.17)	5.75 (1.53)	2.55 (1.12)
intestine	2.35 (1.33)	8.18 (2.32)	19.7 (7.86)	26.38 (5.95)
spleen	2.26 (0.53)	1.56 (0.45)	0.78 (0.26)	0.45 (0.21)
pancreas	5.67(2.72)	2.24 (0.68)	1.40 (0.44)	0.39 (0.29)
heart	6.04 (0.38)	2.77 (0.94)	1.21 (0.66)	0.66 (0.57)
stomach[b]	1.71 (0.38)	5.65 (6.63)	5.00 (2.83)	6.58 (4.59)
brain	3.69 (0.22)	1.53 (0.31)	0.38 (0.05)	0.16 (0.03)
		[^{125}I]**17**		
blood	2.98 (0.64)	4.62 (2.17)	0.83 (0.64)	0.51 (0.31)
liver	12.95 (3.43)	11.20 (1.51)	8.34 (1.98)	7.70 (3.93)
kidney	11.58 (1.13)	9.66 (2.28)	5.84 (1.79)	2.41 (1.22)
intestine	2.52 (0.39)	7.50 (4.85)	17.95 (7.53)	22.64 (5.89)
spleen	2.26 (0.65)	1.40 (0.23)	0.84 (0.23)	0.56 (0.24)
pancreas	5.51 (0.59)	1.84 (0.44)	0.87 (0.37)	0.79 (0.70)
heart	5.67 (1.02)	2.24 (0.56)	1.40 (0.49)	0.39 (0.68)
stomach[b]	3.29 (1.47)	4.73 (5.14)	7.45 (4.62)	7.61 (5.20)
brain	2.81 (0.19)	2.32 (0.21)	0.18 (0.06)	0.08 (0.04)

[a] Expressed as % injected dose per gram. Each value represents the mean (SD) for 4−5 animals. [b] Expressed as % injected dose per organ.

Biodistribution Experiments. To evaluate brain uptake of the aurone derivatives, biodistribution experiments were performed in normal mice with five radioiodinated aurones ([^{125}I]**9**, [^{125}I]**14**, [^{125}I]**15**, [^{125}I]**16**, and [^{125}I]**17**) (Table 2). Radioactivity after injection of the aurone derivatives penetrated the blood−brain barrier showing excellent uptake ranging from 1.7% to 4.5% ID/g brain at 2 min postinjection, a level sufficient for imaging β-amyloid plaques in the brain. In addition, it displayed good clearance from the normal brain with 0.1−0.4% ID/g at 30 min postinjection. Since normal mice were used for the biodistribution experiments, no Aβ plaques were expected in the young mice; therefore, the washout of probes from the brain should be rapid to obtain a higher signal-to-noise ratio earlier in the AD brain. One way to select a ligand with

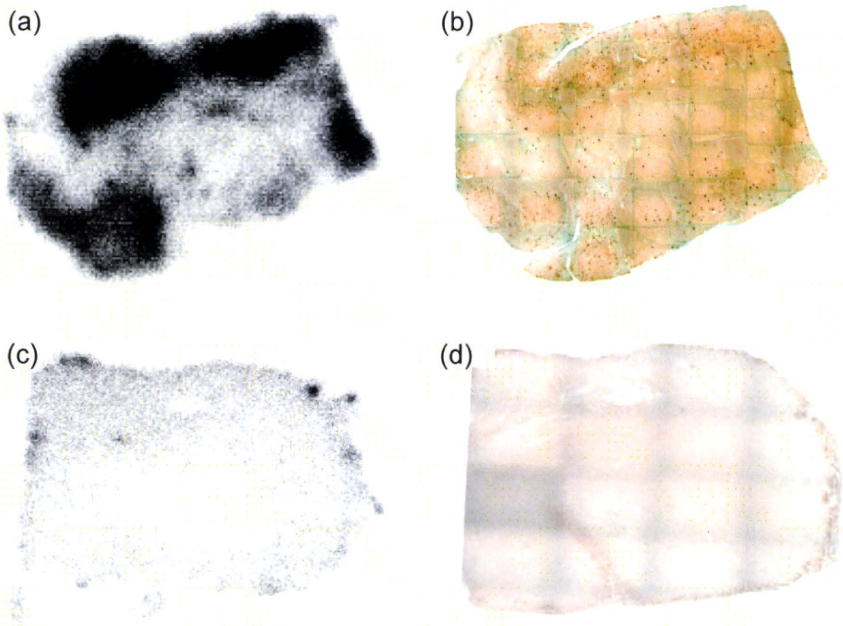

Figure 3. In vitro ARG of [^{125}I]**15** reveals a distinct labeling of amyloid plaques in AD brain sections (a). Under similar conditions, there is very little labeling of [^{125}I]**15** in control brain section (c). The presence and localization of plaques in the sections were confirmed with immunohistochemical staining using a monoclonal Aβ antibody (b, d).

appropriate in vivo kinetics is to use $brain_{2min}/brain_{30min}$ as an index to compare the washout rate. The five radioiodinated aurone derivatives [^{125}I]**9**, [^{125}I]**14**, [^{125}I]**15**, [^{125}I]**16**, and [^{125}I]**17** showed $brain_{2min}/brain_{30min}$ ratios of 15.4, 8.3, 18.8, 9.7, and 15.6, respectively. [^{125}I]**15** had the best washout index. Previously reported radioiodinated aurones showed high uptake (1.9−4.6% ID/g at 2 min postinjection) and good clearance from the brain (0.3−0.5% ID/g at 30 min postinjection) (*19*). However, the $brain_{2min}/brain_{30min}$ ratios of these compounds were 7.3−9.9, lower than that of [^{125}I]**15**, indicating that [^{125}I]**15** could clear more rapidly from the normal mouse brain than aurones with amino groups. It has been reported that [^{123}I]IMPY entered the brain rapidly (2.88% ID at 2 min postinjection) and was cleared from normal brain (0.26% ID at 30 min postinjection), indicating the $brain_{2min}/brain_{30min}$ ratio to be 11.1 (*16*). The aurone derivatives reported in this study appear superior to IMPY in pharmacokinetics, in addition to showing similar binding affinities sufficient for the imaging of β-amyloid plaques in vivo. The pharmacokinetics demonstrated by [^{125}I]**15** is critical to the detection of β-amyloid plaques in the AD brain.

In Vitro Autoradiography. Next, [^{125}I]**15** was investigated for its binding affinity for β-amyloid plaques by in vitro autoradiography in human AD brain sections as shown in Figure 3. Autoradiographic images of [^{125}I]**15** showed high levels of radioactivity in the brain sections (Figure 3a). Furthermore, we confirmed that the hot spots of [^{125}I]**15** corresponded with those of in vitro immunohistochemical staining in the same brain sections (Figure 3b). In contrast, normal human brain displayed no remarkable accumulation of [^{125}I]**15** (Figure 3c), correlating well with the absence of β-amyloid plaques (Figure 3d). These results demonstrate the feasibility of using [^{125}I]**15** as a probe for detecting β-amyloid plaques in the brains of AD patients with SPECT.

CONCLUSION

In conclusion, we successfully designed and synthesized a new series of aurone derivatives as amyloid-imaging agents with high affinity for Aβ(1−42) aggregates in vitro. The derivatives clearly stained amyloid plaques in an animal model of AD, reflecting strong binding to Aβ aggregates in vitro. In biodistribution experiments using normal mice, they displayed good penetration of and fast washout from the brain, especially [^{125}I]**15**. A specific plaque-labeling signal was clearly depicted by [^{125}I]**15** in postmortem AD brain sections. Taken together, the present results suggest [^{125}I]**15** to be a potentially useful probe for the SPECT-based imaging of β-amyloid plaques.

ACKNOWLEDGMENT

This work was supported in part by the Industrial Technology Research Grant Program in 2005 from the New Energy and Industrial Technology Development Organization (NEDO) of Japan and the Program for Promotion of Fundamental Studies in Health Sciences of the National Institute of Biomedical Innovation (NIBIO).

Supporting Information Available: HPLC data of compounds **9**, **14**, **15**, **16**, and **17**. This material is available free of charge via the Internet at http://pubs.acs.org.

LITERATURE CITED

(1) Klunk, W. E. (1998) Biological markers of Alzheimer's disease. *Neurobiol. Aging 19*, 145–7.
(2) Selkoe, D. J. (2001) Alzheimer's disease: genes, proteins, and therapy. *Physiol. Rev. 81*, 741–66.
(3) Selkoe, D. J. (2000) Imaging Alzheimer's amyloid. *Nat. Biotechnol. 18*, 823–4.
(4) Mathis, C. A., Wang, Y., and Klunk, W. E. (2004) Imaging β-amyloid plaques and neurofibrillary tangles in the aging human brain. *Curr. Pharm. Des. 10*, 1469–92.
(5) Nordberg, A. (2004) PET imaging of amyloid in Alzheimer's disease. *Lancet Neurol. 3*, 519–27.
(6) Mathis, C. A., Wang, Y., Holt, D. P., Huang, G. F., Debnath, M. L., and Klunk, W. E. (2003) Synthesis and evaluation of ^{11}C-labeled 6-substituted 2-arylbenzothiazoles as amyloid imaging agents. *J. Med. Chem. 46*, 2740–54.
(7) Klunk, W. E., Engler, H., Nordberg, A., Wang, Y., Blomqvist, G., Holt, D. P., Bergstrom, M., Savitcheva, I., Huang, G. F., Estrada, S., Ausen, B., Debnath, M. L., Barletta, J., Price, J. C., Sandell, J., Lopresti, B. J., Wall, A., Koivisto, P., Antoni, G., Mathis, C. A., and Langstrom, B. (2004) Imaging brain amyloid

in Alzheimer's disease with Pittsburgh compound-B. *Ann. Neurol. 55*, 306–19.

(8) Ono, M., Wilson, A., Nobrega, J., Westaway, D., Verhoeff, P., Zhuang, Z. P., Kung, M. P., and Kung, H. F. (2003) ^{11}C-labeled stilbene derivatives as Aβ-aggregate-specific PET imaging agents for Alzheimer's disease. *Nucl. Med. Biol. 30*, 565–71.

(9) Verhoeff, N. P., Wilson, A. A., Takeshita, S., Trop, L., Hussey, D., Singh, K., Kung, H. F., Kung, M. P., and Houle, S. (2004) In-vivo imaging of Alzheimer disease β-amyloid with [^{11}C]SB-13 PET. *Am. J. Geriatr. Psychiatry 12*, 584–95.

(10) Rowe, C. C., Ackerman, U., Browne, W., Mulligan, R., Pike, K. L., O'Keefe, G., Tochon-Danguy, H., Chan, G., Berlangieri, S. U., Jones, G., Dickinson-Rowe, K. L., Kung, H. P., Zhang, W., Kung, M. P., Skovronsky, D.,'Dyrks, T., Holl, G., Krause, S., Friebe, M., Lehman, L., Lindemann, S., Dinkelborg, L. M., Masters, C. L., and Villemagne, V. L. (2008) Imaging of amyloid beta in Alzheimer's disease with ^{18}F-BAY94-9172, a novel PET tracer: proof of mechanism. *Lancet Neurol. 7*, 129–35.

(11) Kudo, Y., Okamura, N., Furumoto, S., Tashiro, M., Furukawa, K., Maruyama, M., Itoh, M., Iwata, R., Yanai, K., and Arai, H. (2007) 2-(2-[2-Dimethylaminothiazol-5-yl]ethenyl)-6-(2-[fluoro]ethoxy)benzoxazole: A novel PET agent for in vivo detection of dense amyloid plaques in Alzheimer's disease patients. *J. Nucl. Med. 48*, 553–561.

(12) Agdeppa, E. D., Kepe, V., Liu, J., Flores-Torres, S., Satyamurthy, N., Petric, A., Cole, G. M., Small, G. W., Huang, S. C., and Barrio, J. R. (2001) Binding characteristics of radiofluorinated 6-dialkylamino-2-naphthylethylidene derivatives as positron emission tomography imaging probes for β-amyloid plaques in Alzheimer's disease. *J. Neurosci. 21*, RC189.

(13) Shoghi-Jadid, K., Small, G. W., Agdeppa, E. D., Kepe, V., Ercoli, L. M., Siddarth, P., Read, S., Satyamurthy, N., Petric, A., Huang, S. C., and Barrio, J. R. (2002) Localization of neurofibrillary tangles and β-amyloid plaques in the brains of living patients with Alzheimer disease. *Am. J. Geriatr. Psychiatry 10*, 24–35.

(14) Small, G. W., Kepe, V., Ercoli, L. M., Siddarth, P., Bookheimer, S. Y., Miller, K. J., Lavretsky, H., Burggren, A. C., Cole, G. M., Vinters, H. V., Thompson, P. M., Huang, S. C., Satyamurthy, N., Phelps, M. E., and Barrio, J. R. (2006) PET of brain amyloid and tau in mild cognitive impairment. *N. Engl. J. Med. 355*, 2652–63.

(15) Kung, M. P., Hou, C., Zhuang, Z. P., Zhang, B., Skovronsky, D., Trojanowski, J. Q., Lee, V. M., and Kung, H. F. (2002) IMPY: an improved thioflavin-T derivative for in vivo labeling of beta-amyloid plaques. *Brain Res. 956*, 202–10.

(16) Zhuang, Z. P., Kung, M. P., Wilson, A., Lee, C. W., Plossl, K., Hou, C., Holtzman, D. M., and Kung, H. F. (2003) Structure-activity relationship of imidazo[1,2-a]pyridines as ligands for detecting β-amyloid plaques in the brain. *J. Med. Chem. 46*, 237–43.

(17) Newberg, A. B., Wintering, N. A., Plossl, K., Hochold, J., Stabin, M. G., Watson, M., Skovronsky, D., Clark, C. M., Kung, M. P., and Kung, H. F. (2006) Safety, biodistribution, and dosimetry of ^{123}I-IMPY: a novel amyloid plaque-imaging agent for the diagnosis of Alzheimer's disease. *J. Nucl. Med. 47*, 748–54.

(18) Newberg, A. B., Wintering, N. A., Clark, C. M., Plossl, K., Skovronsky, D., Seibyl, J. P., Kung, M. P., and Kung, H. F. (2006) Use of ^{123}I IMPY SPECT to differentiate Alzheimer's disease from controls. *J. Nucl. Med. 47*, 78P.

(19) Ono, M., Maya, Y., Haratake, M., Ito, K., Mori, H., and Nakayama, M. (2007) Aurones serve as probes of β-amyloid plaques in Alzheimer's disease. *Biochem. Biophys. Res. Commun. 361*, 116–21.

(20) Roberts, M., Bentley, M., and Harris, J. (2002) Chemistry for peptide and protein PEGylation. *Adv. Drug Delivery Rev. 54*, 459–76.

(21) Harris, J., and Chess, R. (2003) Effect of pegylation on pharmaceuticals. *Nat. Rev. Drug Discovery 2*, 214–21.

(22) Cheng, Y., and Prusoff, W. (1973) Relationship between the inhibition constant (K1) and the concentration of inhibitor which causes 50% inhibition (I50) of an enzymatic reaction. *Biochem. Pharmacol.* 3099–3108.

(23) Bryant, W., and Huhn, G. (1995) A practical preparation of 7-methoxy-3(2H)-benzofuranone. *Synth. Commun. 25*, 915–20.

(24) Kung, M. P., Hou, C., Zhuang, Z. P., Skovronsky, D., and Kung, H. F. (2004) Binding of two potential imaging agents targeting amyloid plaques in postmortem brain tissues of patients with Alzheimer's disease. *Brain Res. 1025*, 98–105.

(25) Zhang, W., Oya, S., Kung, M. P., Hou, C., Maier, D. L., and Kung, H. F. (2005) F-18 stilbenes as PET imaging agents for detecting β-amyloid plaques in the brain. *J. Med. Chem. 48*, 5980–8.

BC8003292

Eur J Nucl Med Mol Imaging (2010) 37:377–385
DOI 10.1007/s00259-009-1262-2

ORIGINAL ARTICLE

Quantification of regional myocardial oxygen metabolism in normal pigs using positron emission tomography with injectable ^{15}O-O_2

Takashi Temma · Hidehiro Iida · Takuya Hayashi · Noboru Teramoto · Youichiro Ohta · Nobuyuki Kudomi · Hiroshi Watabe · Hideo Saji · Yasuhiro Magata

Received: 27 April 2009 / Accepted: 10 August 2009 / Published online: 4 September 2009

Abstract
Purpose Although ^{15}O-O_2 gas inhalation can provide a reliable and accurate myocardial metabolic rate for oxygen by PET, the spillover from gas volume in the lung distorts the images. Recently, we developed an injectable method in which blood takes up ^{15}O-O_2 from an artificial lung, and this made it possible to estimate oxygen metabolism without the inhalation protocol. In the present study, we evaluated the effectiveness of the injectable ^{15}O-O_2 system in porcine hearts.
Methods PET scans were performed after bolus injection and continuous infusion of injectable ^{15}O-O_2 via a shunt between the femoral artery and the vein in normal pigs. The injection method was compared to the inhalation method. The oxygen extraction fraction (OEF) in the lateral walls of the heart was calculated by a compartmental model in view of the spillover and partial volume effect.
Results A significant decrease of lung radioactivity in PET images was observed compared to the continuous inhalation of ^{15}O-O_2 gas. Furthermore, the injectable ^{15}O-O_2 system provides a measurement of OEF in lateral walls of the heart that is similar to the continuous-inhalation method (0.71 ± 0.036 and 0.72 ± 0.020 for the bolus-injection and continuous-infusion methods, respectively).
Conclusion These results indicate that injectable ^{15}O-O_2 has the potential to evaluate myocardial oxygen metabolism.

Keywords Myocardial oxygen metabolism · PET · Pig · OEF · Injectable ^{15}O-O_2

T. Temma · H. Saji
Department of Patho-Functional Bioanalysis,
Graduate School of Pharmaceutical Sciences, Kyoto University,
Kyoto, Japan

H. Iida · T. Hayashi · N. Teramoto · Y. Ohta · N. Kudomi · H. Watabe
Department of Investigative Radiology,
National Cardiovascular Center Research Institute,
Osaka, Japan

Y. Magata (✉)
Laboratory of Genome Bio-Photonics,
Photon Medical Research Center,
Hamamatsu University School of Medicine,
1-20-1 Handayama,
Hamamatsu 431-3192, Japan
e-mail: magata@hama-med.ac.jp

Introduction

In the myocardium, fatty acid or glucose is used to produce energy by aerobic metabolism. Oxygen is one of the most important substrates closely related to the aerobic metabolism in the TCA cycle; thus, oxygen metabolism should be a direct reflection of myocardial metabolism of these substrates. Therefore, there has been considerable interest in the development of a method to quantify oxygen metabolism in the myocardium.

Recently, ^{11}C-acetate has been used for this purpose [1–5]. ^{11}C-acetate is taken up by the mitochondria and metabolically converted into acetyl-CoA. It then enters the TCA cycle and is transformed to ^{11}C-CO_2, which is cleared rapidly from the myocardium. Thus, the clearance pharmacokinetics reflects oxygen metabolism in the myocardium. However, the quantification of oxygen metabolism using ^{11}C-acetate is quite difficult because of various intermediary compounds.

The use of ^{15}O-O_2 gas inhalation and PET scanning can provide a quantitative myocardial metabolic rate for oxygen ($MMRO_2$) [6, 7]. The tracer kinetic model used is based on that originally proposed to describe the behavior of ^{15}O-O_2 in brain tissue [8, 9]. However, the direct translation of the